



## Design optimization of a polygeneration plant producing power, heat, and lignocellulosic ethanol

Lythcke-Jørgensen, Christoffer Ernst; Haglind, Fredrik

*Published in:*  
Energy Conversion and Management

*Link to article, DOI:*  
[10.1016/j.enconman.2014.12.028](https://doi.org/10.1016/j.enconman.2014.12.028)

*Publication date:*  
2015

*Document Version*  
Peer reviewed version

[Link back to DTU Orbit](#)

*Citation (APA):*  
Lythcke-Jørgensen, C. E., & Haglind, F. (2015). Design optimization of a polygeneration plant producing power, heat, and lignocellulosic ethanol. *Energy Conversion and Management*, 91, 353–366.  
<https://doi.org/10.1016/j.enconman.2014.12.028>

---

### General rights

Copyright and moral rights for the publications made accessible in the public portal are retained by the authors and/or other copyright owners and it is a condition of accessing publications that users recognise and abide by the legal requirements associated with these rights.

- Users may download and print one copy of any publication from the public portal for the purpose of private study or research.
- You may not further distribute the material or use it for any profit-making activity or commercial gain
- You may freely distribute the URL identifying the publication in the public portal

If you believe that this document breaches copyright please contact us providing details, and we will remove access to the work immediately and investigate your claim.

# 1 Design optimization of a polygeneration 2 plant producing power, heat, and 3 lignocellulosic ethanol

---

4 Christoffer Lythcke-Jørgensen<sup>a\*</sup> Fredrik Haglind<sup>b</sup>

5 <sup>a</sup> Technical University of Denmark, Department of Mechanical Engineering, Nils Koppels Allé 403,  
6 DK-2800 Kgs. Lyngby, [celjo@mek.dtu.dk](mailto:celjo@mek.dtu.dk)

7 <sup>b</sup> Technical University of Denmark, Department of Mechanical Engineering, Nils Koppels Allé 403,  
8 DK-2800 Kgs. Lyngby, [frh@mek.dtu.dk](mailto:frh@mek.dtu.dk)

9 \* Corresponding author. +45 30 42 72 00. Email: [celjo@mek.dtu.dk](mailto:celjo@mek.dtu.dk).

## 10 **Abstract**

11 A promising way to increase the energy efficiency and reduce costs of biofuel production is to  
12 integrate it with heat and power production in polygeneration plants. This study treats the  
13 retrofitting of a Danish combined heat and power plant by integrating lignocellulosic ethanol  
14 production based on wheat straw with the aim of minimizing specific ethanol production cost.  
15 Previously developed and validated models of the facilities are applied in the attempt to solve the  
16 design optimization problem. Straw processing capacities in the range of 5 kg/s to 12 kg/s are  
17 considered, while plant operation is optimized over the year with respect to maximal income and  
18 with the limitations that the reference hourly district heating production has to be met while  
19 reference hourly power export cannot be exceeded.

20 The results suggest that the specific ethanol production cost increased continuously from 0.958  
21 Euro/L at a straw processing capacity of 5 kg/s to 1.113 Euro/L at a capacity of 12 kg/s, indicating  
22 that diseconomies-of-scale applies for the suggested ethanol production scheme. A thermodynamic  
23 evaluation further discloses that the average yearly exergy efficiency decreases continuously with  
24 increasing ethanol production capacity, ranging from 0.746 for 5 kg/s to 0.696 for 12 kg/s. This  
25 trend results from operating constraints that induce expensive operation patterns in periods of high  
26 district heating loads or shut-down periods for the combined heat and power plant. A sensitivity  
27 analysis indicates that the found optimum is indifferent to major variations in fossil fuel prices. The  
28 results question the efficiency of the suggested retrofitting scheme in the present energy system, and  
29 they further point towards the importance of taking operating conditions into consideration when  
30 developing flexible polygeneration plant concepts as differences between design-point operation  
31 and actual operation may have a significant impact on overall plant performance.

## 32 **Keywords**

33 Combined heat and power; design optimization; exergy efficiency; lignocellulosic ethanol;  
34 operation optimization; polygeneration

## 35 **Nomenclature**

### 36 **Latin letters**

37	$C$	Cost [Euro]
38	$c$	Specific cost [Euro/GJ]
39	$D$	Dimension [-]
40	$\dot{EX}$	Exergy flow [MJ/h]
41	$ex$	Specific exergy flow [MJ/kg]
42	$I$	Investment [Euro]

43	$M$	Mass [kg]
44	$M_f$	Capacity power factor [-]
45	$\dot{P}$	Power production [MW]
46	$Q$	Heat [MJ]
47	$\dot{Q}$	Heat flow [MJ/s]
48	$\dot{Q}_{fuel}$	Fuel input [MJ/s]
49	$V_{eth}$	Volume ethanol production [L/h]
50	<b>Greek letters</b>	
51	$\alpha$	Back-pressure operation parameter [-]
52	$\beta$	Relative district heating production in the ethanol facility [-]
53	$\eta_{eth}$	Mass efficiency of lignocellulosic-biomass-to-ethanol conversion [-]
54	$\eta_{ex}$	Standard exergy efficiency [-]
55	$\kappa$	Choice between integrated or separate operation [-]
56	$\lambda$	Combined heat and power unit load [-]
57	$\rho$	Density [kg/L]
58	$\sigma$	Straw processing capacity of the ethanol production [kg/s]
59	<b>Subscripts</b>	
60	$add$	Additives
61	$enz$	Enzymes
62	$eth$	Ethanol
63	$i$	Hour of the year
64	$I$	Investment depreciation
65	$O\&M$	Operation and maintenance
66	$ref$	Reference production

67 0 Reference value

68 **Abbreviations**

69 AVV1 Avedøreværket 1

70 CHP Combined Heat and Power

71 DH District Heating

72 L&D (Exergy) Losses and Destruction

73 O&M Operation and Maintenance

74 SSF Simultaneous Saccharification and Fermentation

75 **1. Introduction**

76 Biomass, being the only renewable resource of highly concentrated carbon, is often considered a  
77 cornerstone in renewable energy systems because of its storability and potential conversability to  
78 biofuels with high energy densities [1]. The biomass resource, however, is limited [2], and  
79 competition between food and energy production pose a sustainability challenge [3]. Efficient use  
80 and conversion of sustainably available biomass are therefore of crucial importance in renewable  
81 energy systems [4].

82 Among biofuels, ethanol is presently the most widely used for transportation on a global basis and it  
83 is consumed both as an individual fuel and in blends with gasoline [5]. Ethanol produced from  
84 lignocellulosic biomass is of special interest here because it may yield reduced CO<sub>2</sub> emissions from  
85 transportation without linking fuel prices and food prices directly [4]. Furthermore, ethanol is a  
86 bulk-volume chemical used in industrial and consumer products and lignocellulosic ethanol

87 presents a green chemistry [6]<sup>1</sup> alternative to the existing ethanol production from ethene hydration  
88 or through fermentation of sugars and starch [7]. However, the energy intensive nature of  
89 lignocellulosic ethanol production is a challenge with respect to production efficiency and  
90 economy.

91 In an extensive work on the integrated production of biogas, heat and power based on biomass  
92 gasification, Gassner et Maréchal [8] concluded that biofuel plants may increase energy- and cost-  
93 efficiency simultaneously by applying process systems engineering approaches and by considering  
94 integration with other processes in polygeneration plants (PGPs). Similarly, a promising way to  
95 increase energy- and cost-efficiency of lignocellulosic ethanol production is to integrate it with heat  
96 and power production [4]. Plants integrating the production of power, heat, bio-methane, and  
97 lignocellulosic ethanol have been investigated by several groups, both as grassroot design problems  
98 and retrofit design problems. Regarding grassroot design problems, Daianova et al. [9] and Ilic et al.  
99 [10] both reported better energy economy for integrated PGPs compared to stand-alone production  
100 of the same energy products, assuming constant energy prices over the year. Bösch et al. [11]  
101 discussed how the energy economy of a system producing lignocellulosic ethanol, biogas and  
102 district heating (DH) might be increased by integrating power production. For a similar system,  
103 Modarresi et al. [12] conducted a pinch analysis and reported that heat integration can reduce the  
104 hot and cold utility demands by up to 40%, assuming operation in design point solely. Leduc et al.  
105 [13] conducted a sensitivity analysis of the important parameters for such systems in Sweden and  
106 found that incomes from heat and power sales were the most significant contributors towards  
107 reducing the specific ethanol production costs. With regard to retrofitted systems, Palacios-Bereche

---

<sup>1</sup> Green chemistry consists of environmental friendly, sustainable chemicals and processes the use of which results in reduced waste, safer outputs, and reduced or eliminated pollution and environmental damage [6].

108 et al. [14] studied the integration of lignocellulosic ethanol production in the conventional first-  
109 generation sugarcane ethanol process and reported higher exergy efficiency for the integrated  
110 scheme when considering only design point operation. Lythcke-Jørgensen et al. [15] investigated  
111 the introduction of lignocellulosic ethanol production in an existing combined heat and power  
112 (CHP) and also reported higher exergy efficiencies for integrated operation. In a study of  
113 conversion routes for winter wheat to ethanol, Bentsen et al. [16] suggested that energy savings  
114 could be achieved by integrating lignocellulosic ethanol production in existing CHP units. Starfelt  
115 et al. [17] investigated the integration of lignocellulosic ethanol production in an existing biomass-  
116 based CHP unit in Sweden and concluded that for the same production of heat, power, and ethanol,  
117 the total biomass consumption would be lower for the integrated system than for a separate scenario.  
118 And in a later study, Starfelt et al. [18] concluded that the integration of lignocellulosic ethanol  
119 production in Swedish CHP units with fixed heat-to-power ratios may be profitable if excess heat  
120 capacity is available in the CHP unit for a certain amount of time over the year.

121 In principle, the development and optimization of PGPs can be considered at three levels, similar to  
122 the optimization of energy systems [19] and distributed energy supply systems [20]: Synthesis level,  
123 design level, and operation level. At the synthesis level, the configuration of the PGP is optimized  
124 by either retrofitting an existing plant (retrofit design) or by developing a new plant concept  
125 (grassroot design)<sup>2</sup>, which entails the selection of the desired products and processes. At the design  
126 level, one considers process dimensioning, process integration, required components, and technical  
127 specifications of the equipment. Finally, at the operation level, the operation mode of the given  
128 plant is optimized in the surrounding energy system; this is done by taking expected demands for,  
129 and costs of, energy services and utilities into account as well as interactions with other energy

---

<sup>2</sup> A grassroot design is *a priori* always a solution to a retrofit design optimization problem [20].

130 producers in the system. The operation level is especially important for flexible operating PGPs, e.g.  
131 those set to balance production from intermittent renewable energy sources [21] whenever  
132 economically advantageous [22]. Optimization on operation level has been investigated in literature  
133 for polygeneration plants producing power, heating, cold and fresh water, e.g. in a sequential  
134 optimization methodology presented by Uche et al. [23]. Grisi et al. [24] further illustrated how  
135 commodity market prices may affect operation decisions in a sugarcane biorefinery producing  
136 power, sugar, sugar- and bagasse-based ethanol, and biogas. However, to the authors' best  
137 knowledge the impact of flexible plant operation on economic performance has not been treated  
138 comprehensively in previous studies of the integrated production of power, heat, and lignocellulosic  
139 ethanol.

140 This study assesses the impact on economic and thermodynamic performance of integrating  
141 lignocellulosic ethanol production with flexible heat and power production. The study treats a  
142 retrofit design problem where lignocellulosic ethanol production using the hydrothermal  
143 pretreatment technology IBUS [25]<sup>3</sup> is sought integrated into the Danish CHP unit Avedøreværket 1  
144 (AVV1). The system has previously been studied by the authors and the outcomes suggested that  
145 operating conditions may have a significant impact on both economy [26] and overall exergy  
146 efficiency [27] [15] of the ethanol production. This work builds upon the previous study by  
147 optimizing the PGP at design and operation levels and simultaneously attempting to minimize the  
148 break-even specific ethanol production costs. For each solution to the design problem, the  
149 thermodynamic performance of the ethanol production is further evaluated by applying exergy  
150 analysis [28] and calculating the average exergy efficiency of the ethanol production over the year.

---

<sup>3</sup> IBUS (Integrated Biomass Utilization System) is a patented cellulosic biomass pretreatment technology. The patent is owned by the Danish company Inbicon A/S, a subsidiary to DONG Energy.



151 In this paper, the modelling approach and outcomes of previous studies are given in Section 2. The  
152 design optimization scheme and the thermodynamic performance evaluation method are presented  
153 in Section 3. The outcomes are presented in Section 4 and discussed in Section 5. Finally, Section 6  
154 contains a conclusion of the findings.

## 155 **2. System description and previous work**

### 156 **2.1. System description**

157 The design optimization problem treated in this study concerns the integration of lignocellulosic  
158 ethanol production based on IBUS technology in the existing Danish combined heat and power unit  
159 Avedøreværket 1. A simplified layout of the PGP is presented in Figure 1. A thorough description  
160 of the plant synthesis and modelling, including choice of performance parameters and modelling  
161 validation, is presented in Lythcke-Jørgensen et al. [15].

162 Avedøreværket 1 (AVV1), which was commissioned in 1990, has a net electric power generation in  
163 condensation mode of 250 MW, and of 212 MW in full back pressure mode with a district heating  
164 (DH) production of 330 MJ/s (drive temperature/return temperature 100<sup>0</sup>C/50<sup>0</sup>C) [29]. Part-load  
165 operation in the CHP unit is governed by sliding-pressure control [30]. A numerical model of  
166 AVV1, developed by Elmegaard and Houbak [29] in the energy system simulator Dynamic  
167 Network Analysis [31], was used for simulating flows and operation of the CHP unit.

168 An ethanol production facility based on IBUS technology produces lignocellulosic ethanol, solid  
169 biofuel, and molasses from wheat straw. In the facility, the lignocellulosic structure of the straw is  
170 broken down through treatment with pressurized steam in the hydrothermal pretreatment stage,  
171 whereupon the straw-steam mixture is split into a fiber fraction and a liquid fraction. The fiber  
172 fraction is liquefied by glucose-forming enzymes before fermentation is initiated in simultaneous  
173 fermentation and saccharification (SSF) tanks. Ethanol is distilled from the resulting fermentation

174 broth, leaving a fiber stillage which is treated in various separation stages alongside the  
175 pretreatment liquid fraction, yielding a solid biofuel fraction, a molasses fraction, and a waste water  
176 fraction. The molasses fraction can be used in anaerobic fermentation to produce biogas [12] or as  
177 animal feed [32], while the solid biofuel can be used for combustion or gasification. A model of the  
178 ethanol facility based on heat and mass balances over each of the system processes was developed  
179 in the software Engineering Equation Solver (EES) [33] using the layout reported by Larsen et al.  
180 [32] and Østergaard Petersen et al. [34]. The flows of yeast and enzymes were neglected in mass  
181 balance calculations as they were found to be insignificant. The mass conversion efficiencies for the  
182 ethanol facility products are presented in Table 1.

## 183 **2.2. Outcomes of previous work**

184 In the previous studies of the polygeneration plant, a fixed design was applied to the system in  
185 which the ethanol facility was dimensioned to process all locally available winter wheat straw  
186 within a distance of 50 km from the plant, yielding a straw processing capacity of 6.22 kg/s all year  
187 round. Because of load transition times of more than 180 hours in the ethanol production facility  
188 [34], load changes and stop-and-go operation were not considered feasible and full-load operation  
189 was therefore assumed for the whole year. As the CHP unit was operated according to flexible  
190 power and heat demands, the ethanol production in the PGP could be run in two ways: Integrated  
191 mode or separate mode. In integrated mode, steam extracted from turbines of the CHP unit was  
192 used for covering the hot utility demand of the ethanol facility. During integrated operation, DH  
193 production from the IBUS facility was prioritized over DH production from the CHP unit. In  
194 separate mode, a natural gas boiler with a first law energy efficiency of  $\eta_{boiler} = 0.96$  [35] was  
195 used for generating the steam required by the ethanol facility, and DH production in the ethanol  
196 facility was not considered. The principles of the two PGP operation modes are outlined in Figure 2.

197 In Lythcke-Jørgensen et al. [26], a combined pinch analysis [36] and exergy analysis [28] was  
198 carried out to identify the minimum hot and cold utility demands in the ethanol facility as well as  
199 the steam extraction pattern with the lowest exergy destruction during integrated mode operation. A  
200 10K pinch temperature difference was used, as suggested by Modarresi et al. [12] for a similar  
201 facility. The resulting specific hot and cold utility demands and power consumption of the ethanol  
202 production per kilogram of biomass treated are presented in Table 2.

203 As regards existing steam extraction points in AVV1 only, the optimal integration solution involved  
204 steam extraction from the points marked (A), (B), and (C) in Figure 1. The thermodynamic states of  
205 steam in the three points are summarized in Table 3. Steam for hydrothermal pretreatment was  
206 extracted from node (B) in AVV1 at CHP loads above 0.6, and from node (A) at CHP loads below  
207 0.6. The steam for hydrothermal pretreatment was conditioned in the heat integration network to  
208 meet the exact temperature and pressure requirements of the hydrothermal pretreatment component,  
209 195°C and 13bar [37]. Heat released from steam conditioning was used internally in the ethanol  
210 facility. The remaining hot utility demand of the ethanol facility was covered by steam extracted  
211 from node (C). Condensate from the heat integration network is recycled to the condenser of AVV1  
212 where additional desalinated water is added to compensate for the loss of steam to the hydrothermal  
213 pretreatment. Cooling in the heat integration network is provided by sea water and by DH water  
214 when DH production is activated in the ethanol facility.

215 The energy economy of the PGP was evaluated in Lythcke-Jørgensen et al. [26]. Considering the  
216 PGP as a substitute to AVV1 in the existing Danish energy system and assuming hour-wise quasi-  
217 static operation, the plant was set to produce the same hourly amounts of heat and power as the  
218 CHP unit delivered in 2011, the chosen reference year. Separate operation occurred in periods with  
219 high power demands where steam extraction for driving the ethanol production was not available  
220 and in periods where the CHP unit was shut down. The results suggested that on an average the

221 specific energy cost for the ethanol production could be more than eight times higher during  
222 separate operation than during integrated operation, and that it might be economically advantageous  
223 to optimize the operation pattern of the PGP towards a longer duration of integrated operation. A  
224 scatter distribution of the hour-wise quasi-static operation points for the reference operation is  
225 presented in Figure 3. It should be noted that separate operation occurred for 2060 hours of the year  
226 due to CHP shut-down.

227 Two other studies by Lythcke-Jørgensen et al. [27] [15] investigated six different operation points  
228 for the reference PGP and found that within these, the exergy efficiency of the ethanol production  
229 varied from 0.564 to 0.855. The highest exergy efficiency was obtained for integrated operation  
230 with full DH production in the ethanol facility and lowest possible load in the CHP unit, while the  
231 lowest exergy efficiency was obtained for separate operation. The reason for the large differences in  
232 exergy efficiency was primarily the fact that in integrated operation, low-quality steam was used as  
233 the heat source, while natural gas with a much higher exergy-to-energy ratio was used in separate  
234 operation. These results suggest that integrated operation might be desirable from a thermodynamic  
235 efficiency point-of-view as well.

236 In summary, the previous work on the polygeneration plant suggested that integrated operation was  
237 advantageous compared to separate operation for the following reasons:

- 238     ▪ Energy cost of the ethanol production might be significantly reduced during integrated  
239       operation [26].
- 240     ▪ The exergy efficiency of the straw-to-ethanol conversion was markedly higher for integrated  
241       operation [27] [15].
- 242     ▪ Integrated operation made it possible to run the CHP with lower power production ratios,  
243       which could be advantageous in periods of mandatory DH production and low or negative  
244       power prices [26].

245 The present study seeks to quantify the impact of the suggested benefits by optimizing the design  
246 and operation of the suggested PGP concept.

### 247 **3. Design optimization methodology**

248 The pre-synthesized PGP is optimized simultaneously at the design and operation levels with the  
249 objective of minimizing the break-even specific ethanol production cost. Furthermore, the yearly  
250 average exergy efficiency of the ethanol production is calculated for each solution to the  
251 optimization problem in order to evaluate the efficiency of the ethanol production.

#### 252 **3.1. Economic data**

253 Average costs of the energy commodities coal and gas over the reference year 2011, including  
254 overhead costs, are summarized in Table 4. Information on the market power price in the Denmark  
255 East block for each hour of 2011 was taken from the Nord Pool Spot database [38]. A scatter  
256 distribution showing the maximum, minimum, and average daily power prices is shown in Figure 4.  
257 The average daily power price ranges from 0.153 Euro/kWh to 0.812 Euro/kWh, while the hourly  
258 power price ranges from -0.368 Euro/kWh to 1.902 Euro/kWh. The average yearly power price was  
259 0.494 Euro/kWh.

260 Costs associated with the production of lignocellulosic ethanol in a full scale facility using IBUS  
261 technology, which means a straw processing capacity rate of 1000 tons/day or 11.57 kg/s, were  
262 estimated in a feasibility study by Larsen et al. [32]. The values from the feasibility study were used  
263 as reference values in the present study and are summarized in Table 5.

#### 264 **3.2. Optimization model description**

265 As far as board decisions and substantial investments are concerned, the main parameter for  
266 evaluating a lignocellulosic ethanol production facility is the break-even production cost per liter of

267 ethanol,  $c_{eth}$  [32]. The objective of the optimization problem is to minimize  $c_{eth}$  as perceived by  
 268 the plant owner by varying the design and operation of the plant. The specific ethanol production  
 269 cost is made up of seven cost components: Specific cost for straw  $c_{straw}$ ; specific investment  
 270 depreciation cost  $c_I$ ; specific operation and maintenance (O&M) costs  $c_{O\&M}$ ; specific cost for  
 271 enzymes  $c_{enz}$ ; specific cost for additives  $c_{add}$ ; specific energy costs  $c_{energy}$ ; and specific incomes  
 272 from sales of molasses and solid biofuel  $c_{sales}$ .

$$273 \quad c_{eth} = c_{straw} + c_I + c_{O\&M} + c_{enz} + c_{add} + c_{energy} - c_{sales} \quad (1)$$

### 274 **3.2.1. Decision variables**

275 At *design level*, the previously found optimal integration design [26] with respect to steam  
 276 extraction pattern is kept, while the straw processing capacity of the ethanol production  $\sigma$  is varied.  
 277 The straw processing capacities investigated were set to range from 5 kg/s, being slightly smaller  
 278 than the capacity of the ethanol production in the reference system, to 12 kg/s, which is about the  
 279 size of a full scale IBUS ethanol production facility, as reported by Larsen et al. [32]:

$$280 \quad \sigma \in [5,12] \quad (2)$$

281 At *operation level*, four decision variables are considered for each operation hour  $i$ : The load of the  
 282 CHP unit  $\lambda_i$ , which can be 0.0 or within the range [0.4; 1.0] [29]; the back-pressure operation  
 283 parameter  $\alpha_i$ , which can be varied within the range 0 to 1, with 0 representing condensation mode  
 284 operation and 1 representing full back-pressure operation; the relative production of DH in the  
 285 ethanol facility  $\beta_i$ , which can be varied from 0 to 1; and, finally, a dummy parameter describing the  
 286 choice between integrated and separate operation  $\kappa_i$ , taking the value 1 for integrated operation and  
 287 0 for separate operation.

$$288 \quad 0.40 \leq \lambda_i \leq 1.00 \quad (3)$$

$$289 \quad 0.00 \leq \alpha_i \leq 1.00 \quad (4)$$

290  $0.00 \leq \beta_i \leq 1.00$  (5)

291  $\kappa_i \in \{0,1\}$  (6)

292 No DH production from the ethanol process is considered during separate operation, hence:

293  $\beta_i = 0 \mid \kappa_i = 0.$  (7)

### 294 3.2.2. Constraints

295 As in the previous studies, the plant is seen as a substitute to AVV1 in the present Danish energy  
296 system. As a consequence, two operation constraints were set. Regarding DH production, which is  
297 subject to strict legislation, the PGP was set to deliver the same hour-wise amount of heat  $Q_i$  over  
298 the year as the CHP unit produced in the reference operation,  $Q_{i,ref}$ :

299  $Q_i(\sigma, \lambda_i, \alpha_i, \beta_i, \kappa_i) = Q_{i,ref} \quad \forall i$  (8)

300 With regard to power exports  $P_i$ , the plant is allowed to reduce its export in a given hour compared  
301 to the reference power export  $P_{i,ref}$  as back-up capacity is assumed available in the grid. However,  
302 the plant is not allowed to exceed its reference power export in any hour as it is uncertain whether  
303 or not there would be buyers for the extra power in the grid at the given price.

304  $P_i(\sigma, \lambda_i, \alpha_i, \beta_i, \kappa_i) \leq P_{i,ref} \quad \forall i$  (9)

305 Full hour-wise operation flexibility is assumed for the plant, which means that the choice of  
306 parameters in an hour  $i + 1$  is independent of the choice of parameters in the preceding hour  $i$ .

### 307 3.2.3. Model equations

308 The cost for straw  $c_{straw}$  depends on several factors, such as cultivation soil type, crop type,  
309 irrigation, farm size, transportation distance, production type (organic or non-organic), etc. [39].

310 Especially transportation costs are relevant if one considers a plant processing locally distributed  
311 biomass. However, as the plant in question is located next to the sea on one side and the city of  
312 Copenhagen on the other, straw would most likely have to be imported from other regions, and

313 transportation costs are therefore assumed to be independent of the processing capacity of the  
 314 ethanol production. A study by the Danish Energy Agency, Ea Energianalyse, and Wazee [39]  
 315 estimated that the total cost of straw  $C_{straw}$  for energy purposes in Denmark in 2011 was in the  
 316 range of 48.6-52.5 Euro/ton. To represent the expected higher transportation costs from importing  
 317 straw from the countryside, the highest straw price of  $C_{straw} = 52.5 \text{ Euro/ton}$  was used in this  
 318 study. The specific cost of straw per produced liter of ethanol  $c_{straw}$  was calculated according to  
 319 the following equation:

$$320 \quad c_{straw} = \frac{\eta_{eth}}{\rho_{eth}} C_{straw} \quad (10)$$

321 In this equation,  $\eta_{eth}$  is the mass-based conversion efficiency of straw to ethanol in the PGP, as  
 322 presented in Table 1, while  $\rho_{eth} = 785.5 \text{ m}^3/\text{ton}$  is the ethanol density taken from the software  
 323 Engineering Equation Solver (EES) [33] for a temperature of  $15^\circ\text{C}$  and a pressure of 1bar.

324 The specific depreciation cost for the ethanol production,  $c_I$ , is assumed to be derived from a fixed  
 325 annual depreciation rate, which is directly proportional to the investment cost of the equipment. It is  
 326 common to apply power laws [40] to calculate the investment cost  $I(D)$  of equipment as a function  
 327 of the equipment dimension  $D$ :

$$328 \quad I(D) = I_0 \left( \frac{D}{D_0} \right)^{M_f} \quad (11)$$

329 In the equation,  $I_0$  is the investment in a piece of equipment with the base dimension  $D_0$ , and  $M_f$  is  
 330 a scaling constant that depends on the type of equipment. Assuming that a capacity power law  
 331 exists for the entire ethanol facility with a scaling constant  $M_f$ , the specific depreciation cost for a  
 332 facility of capacity  $\sigma$ ,  $c_I(\sigma)$ , is calculated using the following relation:

$$333 \quad c_I(\sigma) = \left( \frac{\sigma_0}{\sigma} \right) c_{I,0} \left( \frac{\sigma}{\sigma_0} \right)^{M_f} \quad (12)$$



334 Here,  $c_{I,0}$  is the reference depreciation cost presented in Table 5, and  $\sigma_0 = 11.57 \text{ kg/s}$  is the  
 335 reference straw processing capacity. In this study, a scaling constant of  $M_f = 0.7$  is used, as  
 336 suggested by Ilic et al. [10] for a similar facility.  
 337 Similar to the calculation of the investment, a capacity power law relationship with the same scaling  
 338 constant  $M_f$  is assumed to apply when calculating the specific O&M cost,  $c_{O\&M}$ :

$$339 \quad c_{O\&M}(\sigma) = \left(\frac{\sigma_0}{\sigma}\right) c_{O\&M,0} \left(\frac{\sigma}{\sigma_0}\right)^{M_f} \quad (13)$$

340 In the equation,  $c_{O\&M,0}$  is the reference O&M cost associated with a facility of the size  $\sigma_0$ .  
 341 The specific energy cost of the ethanol production  $c_{energy}$  represents the extra energy costs from  
 342 operating the PGP compared to the CHP over the reference year, divided by the PGP ethanol  
 343 production. It consists of three components: Specific cost of extra CHP fuel (coal)  $c_{fuel}$ , specific  
 344 cost of natural gas  $c_{gas}$ , and specific cost of power  $c_{power}$ :

$$345 \quad c_{energy} = c_{fuel} + c_{gas} + c_{power} \quad (14)$$

346 Incomes from DH sales are not associated with the ethanol production as the PGP is set to deliver  
 347 the same amounts of heat on an hourly basis as the CHP unit in the reference year. Furthermore,  
 348 costs for external cooling are negligible because of the ready availability of sea water.  
 349 The CHP fuel cost for an hour  $i$ ,  $c_{fuel,i}$ , is calculated as the difference in fuel cost between the  
 350 chosen operation and the fuel cost for the reference operation:

$$351 \quad c_{fuel,i}(\lambda_i) = \frac{(Q_{fuel,i}(\lambda_i) - Q_{fuel,i,ref}(\lambda_{i,ref})) \cdot c_{coal}}{V_{eth}} \quad (15)$$

352 Here,  $\lambda_{i,ref}$  is the reference CHP unit load,  $Q_{fuel,i}(\lambda_i)$  is the actual fuel consumption of the CHP  
 353 unit,  $Q_{fuel,i,ref}(\lambda_{i,ref})$  is the reference fuel consumption of the CHP unit,  $c_{coal}$  is the specific coal  
 354 cost as given in Table 4, and  $V_{eth}$  is the hourly ethanol production volume calculated as

$$355 \quad V_{eth} = \sigma \cdot \frac{\eta_{eth}}{\rho_{eth}} \cdot 3600s/h \quad (16)$$

356 Natural gas is consumed only during separate operation. The cost of natural gas in an hour  $i$  is a  
 357 function of the straw processing capacity  $\sigma_j$  and the choice of integrated or separate operation  $\kappa_i$ .

$$358 \quad c_{NG,i}(\sigma, \kappa_i) = (1 - \kappa_i) \cdot \left[ \sigma \left( \frac{q_{steam} + q_{heat}}{\eta_{boiler}} \right) \cdot c_{NG} \right] \quad (17)$$

359 Here,  $q_{steam} + q_{heat}$  is the total specific heating demand of the ethanol facility,  $\eta_{boiler} = 0.96$  is  
 360 the thermal efficiency of the natural gas boiler and  $c_{NG}$  is the specific cost of natural gas, as given in  
 361 Table 4.

362 The specific cost of power,  $c_{power}$ , represents both the cost of buying power for running the ethanol  
 363 production during separate operation and the costs of lost power sales in integrated operation when  
 364 the power exports of the PGP are lower than the reference power exports of the CHP unit. The  
 365 specific cost of power in an hour  $i$ ,  $c_{power}$ , is calculated as

$$366 \quad c_{power,i}(\sigma, \lambda_i, \alpha_i, \beta_i, \kappa_i) = \frac{[(P_{i,ref} - P_i(\sigma, \lambda_i, \alpha_i, \beta_i, \kappa_i)) + \kappa_i \cdot P_{eth}(\sigma)] \cdot c_{el,i}}{V_{eth}} \quad (18)$$

367 In the equation,  $P_{i,ref}$  is reference power production of the CHP unit,  $P_i$  is the power production of  
 368 the PGP,  $P_{eth}(\sigma)$  is the power consumption of the ethanol production, and  $c_{el,i}$  is the power price in  
 369 a given hour.

370 Using equation (14), the specific energy cost in a given hour  $i$ ,  $c_{energy,i}$ , is then calculated  
 371 according to the following equation:

$$372 \quad c_{energy,i}(\sigma, \lambda_i, \alpha_i, \beta_i, \kappa_i) = \frac{(\lambda_i - \lambda_{i,ref}) \cdot Q_{nom} \cdot c_{coal}}{V_{eth}} + (1 - \kappa_i) \cdot \left[ \sigma \left( \frac{q_{steam} + q_{heat}}{\eta_{boiler}} \right) \cdot c_{NG} \right] +$$

$$373 \quad \frac{[P_{i,ref} - P_i(\sigma, \lambda_i, \alpha_i, \beta_i, \kappa_i)] \cdot c_{el,i}}{V_{eth}} \quad (19)$$

374 The yearly average specific energy cost  $c_{energy}$  is calculated as

$$375 \quad c_{energy}(\sigma, \lambda, \alpha, \beta, \kappa) = \frac{\sum_{i=1}^{8760} c_{energy,i}(\sigma, \lambda_i, \alpha_i, \beta_i, \kappa_i)}{8760} \quad (20)$$

376 For the specific ethanol production costs, it is assumed that the specific cost for enzymes  $c_{enz}$ ,  
 377 additives  $c_{add}$ , and the specific incomes from by-product sales  $c_{sales}$  are independent of the ethanol  
 378 facility capacity and operation of the CHP unit. The reference values presented in Table 5 are used  
 379 for these parameters.

### 380 3.2.4. Objective function minimization

381 Given the equations (1)–(20) for costs and variable constraints, the objective function, which is the  
 382 break-even specific ethanol production cost, is defined as

$$383 \quad c_{eth}(\sigma, \lambda, \alpha, \beta, \kappa) = \frac{\eta_{eth}}{\rho_{eth}} C_{straw} + c_{I,0} \left(\frac{\sigma}{\sigma_0}\right)^{M_f} + c_{O\&M,0} \left(\frac{\sigma}{\sigma_0}\right)^{M_f} + c_{enz} + c_{add} - c_{sales} +$$

$$384 \quad c_{energy}(\sigma, \lambda, \alpha, \beta, \kappa) \quad (21)$$

385 The optimization problem can then be formulated as

$$386 \quad \begin{cases} \min_{\sigma, \lambda, \alpha, \beta, \kappa} [c_{eth}(\sigma, \lambda, \alpha, \beta, \kappa)] \\ \text{subject to constraints:} \\ \text{equations (7), (8)} \\ \text{with variables:} \\ \sigma_j \in [5, 12]; \quad \alpha, \beta \in [0.0, 1.0]; \quad \lambda \in [0.4, 1.0] \\ \kappa \in \{0, 1\} \end{cases} \quad (22)$$

387 Solving the optimization problem (22) will result in the lowest possible break-even specific ethanol  
 388 production cost for the treated PGP under the set conditions.

### 389 3.2.5. Linearization

390 As the PGP unit model is non-linear, the optimization problem (22) becomes non-linear. To  
 391 simplify the calculations, a piece-wise linearization of the model for the integrated PGP operation  
 392 was introduced. The non-linear operational range of the reference PGP, with a straw processing  
 393 capacity of  $\sigma_{ref} = 6.22$  as described in Section 2, is presented in Figure 5, and six key operational  
 394 points are indicated. The operational characteristics of the six key operation points are described in  
 395 Table 6.

396 The difference in power exports between points (1) and (a) is a direct consequence of the extraction  
 397 of steam and the consumption of produced power to run the ethanol facility in integrated mode. As  
 398 the steam extraction and power consumption are both linear functions of the ethanol facility  
 399 capacity  $\sigma$ , the difference in power yield is assumed to be a linear function of  $\sigma$  as well:

$$400 \quad \dot{P}_1(\sigma) = \dot{P}_a + \sigma \frac{(\dot{P}_{1,PGP,ref} - \dot{P}_a)}{\sigma_{ref}} = 249.3 - 3.54 \cdot \sigma \quad [MW] \quad (23)$$

401 Point (2) relates to point (a) in the sense that the CHP unit is operated in the same way, but with the  
 402 difference that full ethanol DH production is activated. The maximum DH production from the  
 403 ethanol facility is a linear function of the straw processing capacity  $\sigma$ , and the reduced power  
 404 production potential is assumed to be a linear function of  $\sigma$  as well:

$$405 \quad \dot{Q}_2(\sigma) = \sigma \frac{\dot{Q}_{2,PGP,ref}}{\sigma_{ref}} = 13.07 \cdot \sigma \quad [MJ/s] \quad (24)$$

$$406 \quad \dot{P}_2(\sigma) = \dot{P}_a + \sigma \frac{(\dot{P}_{2,PGP,ref} - \dot{P}_a)}{\sigma_{ref}} = 249.3 - 3.99 \cdot \sigma \quad [MW] \quad (25)$$

407 Point (4) relates to point (c) in a similar way as (2) to (a), while (3) relates to (b) and (6) relates to  
 408 (d). Using the same approach for these points, the following relations were obtained for heat and  
 409 power yields in each of the points as a function of  $\sigma$ :

$$410 \quad \dot{Q}_3(\sigma) = \dot{Q}_b + \sigma \frac{(\dot{Q}_{3,PGP,ref} - \dot{Q}_b)}{\sigma_{ref}} = 332.9 + 1.00 \cdot \sigma \quad [MJ/s] \quad (26)$$

$$411 \quad \dot{P}_3(\sigma) = \dot{P}_b + \sigma \frac{(\dot{P}_{3,PGP,ref} - \dot{P}_b)}{\sigma_{ref}} = 216.0 - 3.06 \cdot \sigma \quad [MW] \quad (27)$$

$$412 \quad \dot{Q}_4(\sigma) = \dot{Q}_c + \sigma \frac{(\dot{Q}_{4,PGP,ref} - \dot{Q}_c)}{\sigma_{ref}} = 163.1 + 2.30 \cdot \sigma \quad [MJ/s] \quad (28)$$

$$413 \quad \dot{P}_4(\sigma) = \dot{P}_c + \sigma \frac{(\dot{P}_{4,PGP,ref} - \dot{P}_c)}{\sigma_{ref}} = 86.3 - 1.86 \cdot \sigma \quad [MW] \quad (29)$$

$$414 \quad \dot{Q}_5(\sigma) = \dot{Q}_c + \sigma \frac{(\dot{Q}_{5,PGP,ref} - \dot{Q}_c)}{\sigma_{ref}} = 163.1 - 8.92 \cdot \sigma \quad [MJ/s] \quad (30)$$

$$415 \quad \dot{P}_5(\sigma) = \dot{P}_c + \sigma \frac{(\dot{P}_{5,PGP,ref} - \dot{P}_c)}{\sigma_{ref}} = 86.3 - 1.68 \cdot \sigma \quad [MW] \quad (31)$$

$$416 \quad \dot{P}_6(\sigma) = \dot{P}_d + \sigma \frac{(\dot{P}_{6,PGP,ref} - \dot{P}_d)}{\sigma_{ref}} = 104.9 - 2.40 \cdot \sigma \quad [MW] \quad (32)$$

417 It is furthermore assumed that for a PGP with straw processing capacity  $\sigma$ , the maximum and  
 418 minimum potential power productions in integrated operation,  $\dot{P}_{max}$  and  $\dot{P}_{min}$ , are piece-wise linear  
 419 functions of the heat production  $\dot{Q}$  between the key operation points according to the following  
 420 relations:

$$421 \quad \dot{P}_{max}(\dot{Q}, \sigma) = \begin{cases} \dot{P}_1(\sigma) + \dot{Q} \left( \frac{\dot{P}_2(\sigma) - \dot{P}_1(\sigma)}{\dot{Q}_2(\sigma) - \dot{Q}_1(\sigma)} \right) & | \quad \dot{Q} \in [\dot{Q}_1(\sigma), \dot{Q}_2(\sigma)] \\ \dot{P}_2(\sigma) + (\dot{Q} - \dot{Q}_2(\sigma)) \left( \frac{\dot{P}_3(\sigma) - \dot{P}_2(\sigma)}{\dot{Q}_3(\sigma) - \dot{Q}_2(\sigma)} \right) & | \quad \dot{Q} \in ]\dot{Q}_2(\sigma), \dot{Q}_3(\sigma)] \end{cases} \quad (33)$$

$$422 \quad \dot{P}_{min}(\dot{Q}, \sigma) = \begin{cases} \dot{P}_6(\sigma) + \dot{Q} \left( \frac{\dot{P}_5(\sigma) - \dot{P}_6(\sigma)}{\dot{Q}_5(\sigma) - \dot{Q}_6(\sigma)} \right) & | \quad \dot{Q} \in [\dot{Q}_6(\sigma), \dot{Q}_5(\sigma)] \\ \dot{P}_5(\sigma) + (\dot{Q} - \dot{Q}_5(\sigma)) \left( \frac{\dot{P}_4(\sigma) - \dot{P}_5(\sigma)}{\dot{Q}_4(\sigma) - \dot{Q}_5(\sigma)} \right) & | \quad \dot{Q} \in ]\dot{Q}_5(\sigma), \dot{Q}_4(\sigma)] \\ \dot{P}_4(\sigma) + (\dot{Q} - \dot{Q}_4(\sigma)) \left( \frac{\dot{P}_3(\sigma) - \dot{P}_4(\sigma)}{\dot{Q}_3(\sigma) - \dot{Q}_4(\sigma)} \right) & | \quad \dot{Q} \in ]\dot{Q}_4(\sigma), \dot{Q}_3(\sigma)] \end{cases} \quad (34)$$

423 Evaluating the piece-wise linearized model (23)-(34) for the PGP with the reference straw  
 424 processing capacity, the deviation of the power values between the key operation points was found  
 425 to be in the range of -0.69% to +0.77% when compared to the non-linear thermodynamic model.  
 426 The load  $\lambda$  of the CHP unit on the line between the points (3) and (4) in Figure 5 is seen as a linear  
 427 function of the heat production  $\dot{Q}$  as well:

$$428 \quad \lambda(\dot{Q}) = \lambda_3 + (\dot{Q} - \dot{Q}_3(\sigma)) \frac{(\lambda_4 - \lambda_3)}{(\dot{Q}_4(\sigma) - \dot{Q}_3(\sigma))} = 1 - 0.6 \frac{(\dot{Q} - \dot{Q}_3(\sigma))}{(\dot{Q}_4(\sigma) - \dot{Q}_3(\sigma))} \quad | \quad \dot{Q} \in [\dot{Q}_4(\sigma), \dot{Q}_3(\sigma)] \quad (35)$$

429 The linearization (35) was found to have an accuracy of -0.00% to 3.0% as compared to the non-  
 430 linear thermodynamic model.

431 Finally, the fuel consumption of the CHP unit as a function of the load  $\lambda$ ,  $Q_{fuel}(\lambda)$ , was linearized  
 432 using the linear trendline-function in Microsoft Excel:

$$433 \quad Q_{fuel,i}(\lambda_i) = 1798.7 \cdot \lambda_i + 367.8 \quad [GJ/h] \quad (36)$$

434 The coefficient of determination for the approximated equation (36) was found to be 0.9998 when  
435 compared to the fuel consumption predicted in the thermodynamic model of the CHP unit.

436 Applying (23)-(36) and taking the optimization constraints into account, the optimal operation  
437 solution space is reduced *a priori* to the following four operation points for each hour.

438 1) Integrated operation with maximum power delivery

439 2) Integrated operation with minimum power delivery

440 3) Separate operation with maximum power delivery

441 4) Separate operation with zero CHP load

442 The reasoning is that under the given assumptions, separate operation is advantageous only when  
443 the cost of lost power sales is higher than the cost of natural gas for running the ethanol production.

444 However, for the 2060 hours during which the CHP unit was shut down in the reference scenario,  
445 the PGP is forced to operate in separate mode as well. When integrated operation is advantageous, it  
446 is either optimal to maximize or minimize power production, depending on whether income from  
447 power sales is higher or lower than the cost for CHP fuel.

### 448 3.3. Thermodynamic performance evaluation

449 The thermodynamic performance of any design solution is evaluated by calculating the average  
450 yearly exergy efficiency  $\eta_{ex}$  of the ethanol production:

$$451 \quad \eta_{ex} = \frac{\sum_{i=1}^{8760} \eta_{ex,i}}{8760} \quad (37)$$

452 In eq. (37),  $\eta_{ex,i}$  is the hour-wise exergy efficiency of the ethanol production. Using the exergy  
453 analysis method described in Lythcke-Jørgensen et al. [15] for calculating exergy contents of the  
454 flows in the ethanol production, the hourly exergy efficiency is calculated as

$$455 \quad \eta_{ex,i} = \frac{\sum EX_{products,i}}{\sum EX_{in,i}} \quad (38)$$

456 Here  $\sum \dot{EX}_{in,i}$  is the sum of exergy contents in the power and natural gas or steam into the system  
 457 over the hour  $i$ .  $\sum \dot{EX}_{products,i}$  is the sum of exergy contents in the products delivered over the hour  
 458  $i$ , be it ethanol, molasses, solid biofuel, or, potentially, district heating. The calculated exergy  
 459 contents of biomass flows per kg of biomass treated and the exergy content of the natural gas flow  
 460 during integrated and separate operation are presented in Table 7.

461 The exergy content of the steam extracted from the CHP unit during integrated operation depends  
 462 on the chosen operation mode according to the decision variables  $\{\lambda_i, \alpha_i, \beta_i, \kappa_i\}$ . The exergy content  
 463 of the extracted steam in a given hour  $\dot{EX}_{steam,i}$  was calculated directly in the PGP model, and the  
 464 corresponding specific exergy content per kg of straw treated  $ex_{steam,i}$  was calculated using the  
 465 following equation:

$$466 \quad ex_{steam,i}(\lambda_i, \alpha_i, \beta_i, \kappa_i) = \frac{\dot{EX}_{steam,i}(\lambda_i, \alpha_i, \beta_i, \kappa_i)}{\sigma} \quad (39)$$

## 467 **4. Results**

### 468 **4.1. Cost minimization**

469 When solving the optimization problem (22), the specific ethanol production cost obtained is  
 470 plotted as a function of  $\sigma$  in Figure 6 together with four of the key specific cost components:  
 471 Specific energy costs, specific straw cost, specific O&M costs, and specific investment depreciation  
 472 cost. The lowest specific ethanol production cost,  $c_{eth} = 0.958 \text{ Euro/L}$ , was obtained for  $\sigma =$   
 473  $5 \text{ kg/s}$ . The specific energy cost, on an average  $0.517 \text{ Euro/L}$  over the year for this solution, was  
 474 found to be the largest single post in the total specific ethanol production cost. Average specific  
 475 energy costs were found to be  $0.213 \text{ Euro/L}$  during integrated operation and  $1.192 \text{ Euro/L}$  during  
 476 separate operation for the optimal solution, underlining the economic inefficiency of the separate  
 477 operation. Comparing these costs to an average ethanol price of  $0.55 \text{ Euro/L}$  on the European

478 market in the period 2008-2010 [41], the results suggest that even the optimal design is  
479 uncompetitive, mainly due to the duration of separate operation.

480 An important outcome of the study is the diseconomies-of-scale trend that is found to apply for the  
481 ethanol production costs, which is in contrast to the commonly accepted economies-of-scale  
482 principle. In the present case, the diseconomy-of-scale is directly related to the energy costs of the  
483 production whose increase with increased capacity  $\sigma$  exceeds the capacity-dependent decrease in  
484 specific investment costs and O&M costs, as shown in Figure 6.

485 The increase in specific energy costs with  $\sigma$  was found to be a consequence of changes in the  
486 operation pattern. Figure 7 shows the optimal operation characteristics of the solutions as a function  
487 of  $\sigma$ , and it is seen that the duration of separate operation increases with increased  $\sigma$ . This effect was  
488 caused by high power prices and the reduced power production potential during integrated  
489 operation with increasing  $\sigma$ , causing the cost of lost power sales to exceed the cost of running the  
490 PGP in separate operation for an increasing amount of hours over the year.

491 In Figure 8, this effect is further highlighted by plotting the components of the specific energy cost  
492 as a function of  $\sigma$ . It is seen that the specific costs for power and gas increased with increasing  $\sigma$   
493 because of the longer duration of separate operation, causing the overall specific energy costs to  
494 increase. The specific coal cost is seen to decrease with increased  $\sigma$  owing to the decreased duration  
495 of integrated operation.

496 Another significant outcome with respect to operation is the low duration of integrated operation in  
497 minimum load. As described in Section 2.2, one of the three assumed advantages of the integrated  
498 system was the potential of reducing power production in periods with low or negative power prices.  
499 However, in the East Denmark power block anno 2011, the solution to the optimization problem  
500 (22) found it optimal to use this advantage for only 104h over the year. For the rest of the integrated  
501 operation points, the economical optimization maximized the power production within the set



502 operational constraint (9). This is further evident from the scatter distribution of the optimal quasi-  
503 static hourly operation points for the solution with  $\sigma = 5\text{kg/s}$  shown in Figure 9, where only a few  
504 of the optimal operation points are found on the lower boarder of the feasible operation range. The  
505 main reason for the short use of this advantage is the low coal price and the resultant low break-  
506 even electricity production cost in the CHP unit, making it economically unattractive to minimize  
507 power production unless power prices are very low. What is further worth noticing in Figure 9 is the  
508 gap between the upper boarder of the feasible operation range for integrated operation and the  
509 separate operation points. For the reference operation points located in this gap, the optimization  
510 found that the costs for sustaining integrated operation in terms of lost power sales were lower than  
511 the corresponding energy costs for running separate operation, hence integrated operation was  
512 preferred.

#### 513 **4.2. Thermodynamic performance**

514 The exergy efficiency for the ethanol production in each of the operation points over the year was  
515 calculated. Results for selected operation points are presented in Table 8.

516 It is seen that the exergy efficiency of the ethanol production is significantly higher for integrated  
517 operation than for separate operation, mainly owing to the fact that steam from the CHP unit is  
518 replaced by natural gas, with a very high exergy-to-energy ratio, as the hot utility source during  
519 separate operation. Furthermore, the results suggest that the exergy efficiency is higher when full  
520 district heating production is activated in the ethanol facility because the exergy content of the  
521 waste heat from the processes, which would otherwise be lost to external cooling, is contained in  
522 the product 'district heating'. Finally, the exergy efficiency was found to increase with reduced load  
523  $\lambda_i$  in the intervals 0.4-0.6 and 0.6-1.0. The reason for the increased efficiencies with reduced  $\lambda_i$  is  
524 the fact that the exergy content of the extracted steam decreases with decreased  $\lambda_i$ , as indicated by  
525 the values in Table 3. At loads below 0.6, the steam is extracted in a different pattern than for loads

24

526 of 0.6 or higher in the CHP unit, as explained in Section 2, causing the break in the exergy  
527 efficiency trend at this point.

528 The yearly average exergy efficiency of the ethanol production for the optimal operation pattern as  
529 a function of  $\sigma$  is plotted in Figure 10. The average exergy efficiency is found to decrease with  
530 increased  $\sigma$ , mainly owing to the increased duration of separate operation. The highest yearly  
531 average exergy efficiency of  $\eta_{II} = 0.746$  was obtained for the optimal operation pattern for  
532  $\sigma = 5\text{kg/s}$ .

533 A Grassmann diagram illustrating the yearly average exergy flows in the ethanol production for the  
534 optimal solution,  $\sigma = 5\text{kg/s}$  is presented in Figure 11. It is seen that the main part of exergy losses  
535 and destruction (L&D) occurs in the heat integration network, which is mainly caused by two  
536 factors: The use of high-quality natural gas as heat source in separate operation and the fact that  
537 waste heat is not always used for DH production.

538 Evaluating the simulation results for the optimized solutions, another interesting outcome was  
539 found with respect to thermodynamic performance of the PGP: The increase in CHP coal  
540 consumption in MJ/s during integrated operation was lower than the energy in the extracted steam  
541 in MJ/s to run the ethanol production when DH production was activated in the ethanol facility. The  
542 cause of this phenomenon was the DH production from waste heat in the ethanol facility: It allowed  
543 the CHP unit to reduce the steam extraction from turbines for DH production without  
544 compromising the total DH production, thereby allowing higher levels of power production in the  
545 CHP unit. A similar phenomenon was described for an analogue system by Starfelt et al. [17]. This  
546 suggests that not just the exergy efficiency, but also the overall energy efficiency is higher for the  
547 integrated production of lignocellulosic ethanol.

### 548 **4.3. Sensitivity analysis**

549 As several of the cost values are based on assumptions or approximations, a sensitivity analysis was  
550 carried out for nine parameters in the optimal solution in order to investigate the impact on the  
551 production cost of the break-even specific ethanol production cost. The results are presented in a  
552 spider plot in Figure 12.

553 It is seen that variations in straw price, natural gas price, and the value of the sold by-products will  
554 have the highest impact on the specific ethanol production price. On the other hand, it is also seen  
555 that the break-even specific ethanol production cost is hardly affected by variations in coal price.

556 What is further of interest is the fact that an increase in the power law scaling constant will reduce  
557 the specific ethanol production cost because the capacity of the optimal solution is smaller than the  
558 reference capacity; a higher capacity power factor will therefore limit the increases in specific costs  
559 for O&M and depreciation for the smaller facility.

560 Although having the highest impact on specific ethanol production costs, the straw price does not  
561 affect the optimal dimension of the ethanol facility, as it is kept constant. Furthermore, as seen in  
562 Figure 6, O&M, investment and depreciation costs were less significant than specific energy costs  
563 when determining the optimal dimension. As historical data were used for power price and heat  
564 demand, it was investigated if changes in the assumed coal and natural gas prices would affect the  
565 optimal dimension. However, varying the value of each of the parameters from 0% to 1000% of the  
566 assumed value, the optimal design remained unchanged. This suggests that the diseconomy-of-scale  
567 trend identified prevails even in case of major changes in fuel costs occurred.

### 568 **5. Discussion**

569 For the PGP treated in this study, integrated operation was found to be advantageous when  
570 compared to separate operation as it achieved a lower specific energy cost, a higher first law energy

571 efficiency for the entire PGP, when district heating production was activated in the ethanol facility,  
572 and a higher ethanol production exergy efficiency. These outcomes all comply with results reported  
573 by other studies on integrating lignocellulosic ethanol in CHP units. As a consequence, the expected  
574 long duration of separate operation over the year even for the optimal solution poses a major  
575 challenge for the ambition of reducing the costs of lignocellulosic ethanol production by integrating  
576 it with the CHP plant. The duration of separate operation over the year was found to increase with  
577 increased straw processing capacity  $\sigma$  of the ethanol facility, resulting in a diseconomy-of-scale  
578 trend for the suggested integration scheme. This trend was caused by the reduced power production  
579 potential with increased  $\sigma$  for integrated PGP operation, often making the cost of lost power sales  
580 exceed the costs of the inefficient separate operation.

581 For the optimal solution, separate operation occurred for 2718h over the year, of which the 2060h  
582 were caused by CHP unit down-time. The simplest way to increase the duration of integrated  
583 operation would be to reduce the duration of CHP unit down-time. Whether this is feasible for the  
584 given CHP unit is uncertain, but in general it underlines the importance of considering integration  
585 availability when integrating biomass-conversion processes in CHP units, a topic also discussed by  
586 Kohl et al. [42]. It should be mentioned here that the choice of reference year has a significant  
587 impact on the outcomes, as abnormalities in the chosen reference year affect the overall evaluation  
588 results. Whether or not 2011 is suitable as a reference year for the suggested polygeneration scheme  
589 should be investigated further before any final conclusion can be drawn with respect to the  
590 competitiveness of the suggested scheme. For instance, Starfelt et al. [18] considered a down-time  
591 of only 326h for a CHP unit in their study, which however was the sole producer of heat in a local  
592 district heating network. Opposed to this, AVV1 competes with other heat producers in the greater  
593 Copenhagen district heating network, so the prolonged down-time could be a result of economic  
594 decisions. If so, the decisions may have been altered if ethanol production had been integrated in the

595 CHP unit, which would have provided different options for optimizing operation economy in  
596 otherwise unfavourable market conditions, e.g. by minimizing power production while sustaining  
597 integrated mode operation.

598 When conducting the optimization on design and operation levels, it was assumed that the ethanol  
599 production was to be sustained at full load all year round. However, it might be possible to reduce  
600 the duration of separate operation if the load could be varied in the ethanol production, or if the  
601 straw pretreatment could be performed in batches. This would allow integrated operation during  
602 periods of lower power demands and no pretreatment during periods of high power demands,  
603 thereby significantly increasing the power production potential in integrated operation.

604 Furthermore, the energy demands of the separation stage could possibly be reduced by applying  
605 state-of-the-art mechanical separation technologies. It is, however, beyond the scope of the present  
606 paper to evaluate whether or not these suggestions are technologically feasible.

607 Another assumption during the optimization was the constraint that the PGP had to meet the heat  
608 production of the reference CHP unit for each hour of the year. If sufficient heat storage capacity  
609 was available, it might be possible to relax this constraint by assuming that the total production over  
610 a period of 24h had to be met instead of the hour-wise production. This would allow operation  
611 flexibility within the 24h periods and, potentially, longer durations of integrated operation over the  
612 year as well.

613 A simplification of the calculations entailed the assumption of constant biomass price independently  
614 of the processing capacity of the ethanol production. However, this assumption may not be valid for  
615 at least two reasons: Firstly, transportation costs will most likely increase with increased biomass  
616 consumption due to the distributed nature of straw, the biomass processed in this system [43]. And  
617 secondly, large-scale consumption of straw would induce competition with other straw-consumers  
618 causing straw prices to increase further. Such developments in the straw price might increase the

619 diseconomies-of-scale trend for the costs of the integrated ethanol production. A more robust straw  
620 cost calculation model, taking into account the straw supply chain and competing uses, is a topic of  
621 future research for the authors.

622 One of the benefits of the suggested PGP is its ability to reduce the power production without  
623 compromising heat production during periods of low or negative power prices. For the optimal  
624 solution, this advantage was exploited for 104h over the year of 2011. In the future, this advantage  
625 may become more pronounced as an increased production from intermittent renewable energy  
626 sources is integrated in the energy system, increasing the demand for balancing means in the heat-  
627 and-power sectors [1] and potentially providing another *raison d'être* for the PGP. However, in  
628 order to predict the development of the energy system, advanced energy system analysis methods  
629 [44] should preferably be applied. Integration of energy system analysis with the synthesis, design,  
630 and operation optimization of PGPs is another topic for future research for the authors.

631 Concludingly, the results of the study point towards two overall outcomes: Firstly, they question the  
632 efficiency of integrating lignocellulosic ethanol production in the Danish CHP unit AVV1 in the  
633 present energy system. Secondly, they illustrate how operating conditions may have a significant  
634 impact on plant performance; for the PGP in question, design point operation predicted a specific  
635 energy cost of 0.213 Euro/L ethanol produced and an exergy efficiency in the range 0.842-0.855,  
636 while a performance optimization with respect to expected operating conditions yielded a best-case  
637 average specific energy cost of 0.517 Euro/L ethanol and a yearly average exergy efficiency of  
638 0.746.

## 639 **6. Conclusion**

640 This study treats the simultaneous optimization of design and operation levels for a polygeneration  
641 plant in which hydrothermal pretreatment-based lignocellulosic ethanol production is assumed

642 integrated in the Danish combined heat and power unit Avedøreværket 1. The objective of the  
643 optimization is to minimize the specific ethanol production costs, as perceived by the plant owner.  
644 The optimization considers straw processing capacities in the ethanol production ranging from 5  
645 kg/s to 12 kg/s, and quasi-static hour-wise operation over a year. The polygeneration plant operation  
646 is constrained by a fixed hourly heat production and an upper limit for the hourly power exports.  
647 Capacity power laws are used for predicting specific costs of investment depreciation and operation  
648 and maintenance (O&M), while the energy cost is calculated as a function of the operation over the  
649 year.

650 The results suggests that diseconomies of scale applies to specific ethanol production costs in the  
651 integrated polygeneration plant, with the lowest feasible specific ethanol production cost of 0.958  
652 Euro/L being obtained for the design with the smallest ethanol facility capacity considered. The  
653 cause of the diseconomies-of-scale phenomenon is the high reference power production of the CHP  
654 unit, causing the costs from lost power sales and separate operation to exceed the economies-of-  
655 scale benefits from investment depreciation and O&M when increasing ethanol production capacity.

656 A thermodynamic performance evaluation further indicate that the design with the smallest ethanol  
657 production capacity is optimal in terms of average yearly exergy efficiency of the ethanol  
658 production as well, as it obtains the shortest duration of exergy-wise less efficient separate  
659 operation over the year. A sensitivity analysis indicates that variations in straw price and by-  
660 products value would have the most significant impact on the specific ethanol production costs,  
661 whereas the optimum is indifferent to major variations in fossil fuel prices.

662 In summary, the outcomes of this study question the economic viability and thermodynamic  
663 efficiency of integrating lignocellulosic ethanol production in a combined heat and power unit  
664 under the given conditions. Furthermore, the outcomes point towards the importance of considering  
665 operating conditions when developing flexible polygeneration plant concepts.

666 **Acknowledgements**

667 The authors would like to acknowledge DONG Energy for their financial support of the research,  
668 and Brian Elmegaard for allowing the use of his numerical model of the Danish combined heat and  
669 power unit Avedøreværket 1 in the study.

670 **References**

671

- [1] H. Lund, *Renewable energy systems: the choice and modelling of 100% renewable solutions*, Burlington, USA: Elsevier, 2010.
- [2] O. Edenhofer, R. Pichs-Madruga and Y. Sokona, "Renewable Energy Sources and Climate Change Mitigation," Intergovernmental Panel on Climate Change and Cambridge University Press, New York, USA, 2012.
- [3] J. P. W. Scharlemann and W. F. Laruance, "How green are biofuels?," *Environmental Science*, no. 319, pp. 43-44, 2008.
- [4] M. Gassner and F. Maréchal, "Increasing Efficiency of Fuel Ethanol Production from Lignocellulosic Biomass by Process Integration," *Energy Fuels*, no. 27, pp. 2107-2115, 2013.
- [5] M. Balat, "Production of bioethanol from materials via the biochemical pathway: A review," *Energy Conversion and Management*, no. 52, pp. 858-875, 2010.
- [6] US Environmental Protection Agency, Green Chemistry Programme, "Basic Information," 8 August 2012. [Online]. Available: [http://www.epa.gov/greenchemistry/pubs/basic\\_info.html](http://www.epa.gov/greenchemistry/pubs/basic_info.html). [Accessed 5 August 2013].
- [7] S. Lee and Y. T. Shah, "Ethanol from Lignocellulose," in *Biofuels and Bioenergy: Processes and Technologies*, Boca Raton, Florida, USA, Taylor & Francis Group, 2013, pp. 93-146.



- [8] M. Gassner and F. Maréchal, "Thermo-economic optimisation of the polygeneration of synthetic natural gas (SNG), power and heat from lignocellulosic biomass by gasification and methanation," *Energy & Environmental Science*, no. 5, pp. 5768-5789, 2012.
- [9] L. Daianova, E. Dotzauer, E. Thorin and J. Yan, "Evaluation of a regional bioenergy system with local production of biofuel for transportation, integrated with a CHP plant," *Applied Energy*, no. 92, pp. 739-749, 2011.
- [10] D. D. Ilic, E. Dotzauer and L. Trygg, "District heating and ethanol production through polygeneration in Stockholm," *Applied Energy*, no. 91, pp. 214-221, 2011.
- [11] P. Bösch, A. Modarresi and A. Friedl, "Comparison of combined ethanol and biogas polygeneration facilities using exergy analysis," *Applied Thermal Engineering*, no. 37, pp. 19-29, 2012.
- [12] A. Modarresi, P. Kravanja and A. Friedl, "Pinch and exergy analysis of lignocellulosic ethanol, biomethane, heat and power production from straw," *Applied Thermal Engineering*, no. 43, pp. 20-28, 2012.
- [13] S. Leduc, F. Starfelt, E. Dotzauer, G. Kindermann, I. McCallum, M. Obersteiner and J. Lundgren, "Optimal location of lignocellulosic ethanol refineries with polygeneration in Sweden," *Energy*, no. 35, pp. 2709-2716, 2010.
- [14] R. Palacios-Bereche, K. J. Mosqueira-Salazar, M. Modesto, A. V. Ensinas, S. A. Nebra, L. M. Serra and M.-A. Lozano, "Exergetic analysis of the integrated first- and second-generation ethanol production from sugarcane," *Energy*, no. 62, pp. 46-61, 2013.
- [15] C. Lythcke-Jørgensen, F. Haglind and L. R. Clausen, "Exergy analysis of a combined heat and power plant with integrated lignocellulosic ethanol production," *Energy Conversion and Management*, vol. 85, no. 817-827, 2014.

- [16] N. S. Bentsen, B. j. Thorsen and C. Felby, "Energy, feed and land-use balances of refining winter wheat to ethanol," *Biofuels, Bioproducts & Biorefining*, no. 3, pp. 521-533, 2009.
- [17] F. Starfelt, E. Thorin, E. Dotzauer and J. Yan, "Performance evaluation of adding ethanol production into an existing combined heat and power plant," *Bioresource Technology*, no. 101, pp. 613-618, 2009.
- [18] F. Starfelt, L. Daianova, J. Yan, E. Thorin and E. Dotzauer, "The impact of lignocellulosic ethanol yields in polygeneration with district heating – A case study," *Applied Energy*, no. 92, pp. 791-799, 2012.
- [19] C. A. Frangopoulos, M. R. von Spakovsky and E. Scubba, "A Brief Review of Methods for the Design and Synthesis Optimization of Energy Systems," *International Journal of Applied Thermodynamics*, no. 4, pp. 151-160, 2002.
- [20] P. Voll, M. Lampe, G. Wrobel and A. Bardow, "Superstructure-free synthesis and optimization of distributed industrial energy supply systems," *Energy*, no. 45, pp. 424-435, 2012.
- [21] H. Lund, A. N. Andersen, P. A. Østergaard, B. V. Mathiesen and D. Connolly, "From electricity smart grids to smart energy systems - A market operation based approach and understanding," *Energy*, no. 42, pp. 96-102, 2012.
- [22] Y. Chen, T. A. Adams II and P. I. Barton, "Optimal Design and Operation of Flexible Energy Polygeneration Systems," *Industrial & Engineering Chemistry Research*, no. 50, pp. 4553-4566, 2011.
- [23] C. Rubio-Maya, J. Uche and A. Martínez, "Sequential optimization of a polygeneration plant," *Energy Conversion and Management*, no. 52, pp. 2861-2869, 2011.
- [24] E. F. Grisi, J. M. Yusta and H. M. Khodr, "A short-term scheduling for the optimal operation of biorefineries," *Energy Conversion and Management*, no. 52, pp. 447-456, 2011.

- [25] J. Larsen, M. Østergaard Haven and L. Thirup, "Inbicon makes lignocellulosic ethanol a commercial reality," *Biomass and Bioenergy*, no. 46, pp. 36-45, 2012.
- [26] C. Lythcke-Jørgensen, F. Haglind and L. R. Clausen, "Thermodynamic and economic analysis of integrating lignocellulosic bioethanol production in a Danish combined heat and power plant," in *21st European Biomass Conference & Exhibition*, Copenhagen, Denmark, 2013, June 3-7.
- [27] C. Lythcke-Jørgensen, F. Haglind and L. R. Clausen, "Exergy analysis of a combined heat and power plant with integrated lignocellulosic ethanol production," in *International Conference on Efficiency, Cost, Optimization, Simulation, and Environmental Impact of Energy Systems*, Guilin, China, 2013, July 16-19.
- [28] A. Bejan, G. Tsatsaronis and M. Moran, *Thermal Design & Optimization*, John Wiley & Sons, Inc., 1996.
- [29] B. Elmegaard and N. Houbak, "Simulation of the Avedøreværket Unit 1 cogeneration plant with DNA," in *16th International Conference on Efficiency, Cost, Optimization, Simulation and Environmental Impact of Energy Systems*, Kgs. Lyngby, Denmark, 2003, June 30 - July 2.
- [30] H. Spliethoff, *Power Generation from Solid Fuels*, München, Germany: Springer-Verlag Berlin Heidelberg, 2010.
- [31] B. Elmegaard and N. Houbak, "DNA - A General Energy System Simulation Tool," in *SIMS 2005 : 46th Conference on Simulation and Modeling*, pp. 43-52, Trondheim, Norway, 2005, October 13-14.
- [32] J. Larsen, M. Ø. Petersen, L. Thirup, H. W. Li and F. K. Iversen, "The IBUS Process - Lignocellulosic Bioethanol Close to a Commercial Reality," *Chemical Engineering & Technology*, no. 5, pp. 765-772, 2008.

- [33] "F-Chart Software," [Online]. Available: <http://www.fchart.com/ees/>. [Accessed 25 February 2013].
- [34] M. Østergaard Petersen, J. Larsen and M. Hedegaard Thomsen, "Optimization of hydrothermal pretreatment of wheat straw for production of bioethanol at low water consumption without addition of chemicals," *Biomass and Bioenergy*, no. 33, pp. 834-840, 2009.
- [35] Energistyrelsen, "Technology Data for Energy Plants," Danish Energy Agency, 2010.
- [36] I. C. Kemp, *Pinch Analysis and Process Integration*, 2nd edition, Oxford, UK: Butterworth-Heinemann, 2006.
- [37] N. S. Bentsen, C. Felby and K. H. Ipsen, "Energy Balance of 2nd Generation Bioethanol Production in Denmark," *Elsam A/S*, 2006.
- [38] NordPoolSpot, "Nord Pool Spot," 2011. [Online]. Available: <http://www.nordpoolspot.com/>. [Accessed 22 June 2012].
- [39] Ea Energianalyse, Energistyrelsen, Wazee, "Opdatering af samfundsøkonomiske brændselspriser," Ea Energianalyse, Copenhagen, Denmark, 2011.
- [40] R. Smith, *Chemical Process Design and Integration*, West Sussex, England: John Wiley & Sons Ltd, 2005.
- [41] Statens Energimyndighet, "Energiläget 2011," Statens Energimyndighet, Eskilstuna, Sweden, 2011.
- [42] T. Kohl, T. Laukkanen, M. Järvinen and C.-J. Fogelholm, "Energetic and environmental performance of three biomass upgrading processes integrated with a CHP plant," *Applied Energy*, no. 107, pp. 124-134, 2013.
- [43] M. W. Jack, "Scaling laws and technology development strategies for biorefineries and

bioenergy plants.," *Bioresource Technology*, no. 100, pp. 6324-6330, 2009.

[44] D. Connolly, H. Lund, B. Mathiesen and M. Leahy, "A review of computer tools for analysing the integration of renewable energy in various energy systems," *Applied Energy*, no. 87, pp. 1059-1082, 2010.

672

673

*Table 1 – Mass conversion efficiencies of the products in the modelled ethanol facility.*

Mass conversion efficiency	Nomenclature	Value [-]
Ethanol	$\eta_{eth}$	0.150
Molasses	$\eta_{mol}$	0.371
Solid biofuel	$\eta_{biofuel}$	0.407

Table 2 – Specific energy utility requirements of the ethanol production for operation with zero and full DH production in the ethanol facility.

Utility	Nomenclature	Energy [MJ/kg]		Temperature [°C]	Pressure [bar]
		- zero DH	- full DH		
Steam	$q_{steam}$	5.5	5.5	195	13
Heating	$q_{heat}$	5.7	8.0	>100	-
Cooling	$q_{cool}$	11.5	1.0	<20	-
Power	$p$	0.792 <sup>a</sup>	0.792 <sup>a</sup>	-	-

<sup>a</sup> A constant power consumption of 220 kWh/ton of straw treated was used as suggested by Bentsen et al. [32].

Table 3 – Temperature (T), pressure (P), and specific exergy content (ex) of steam in the extraction points (A), (B), and (C) at various loads.

CHP Load	(A)			(B)			(C)		
	T [C]	P [bar]	ex [kJ/kg]	T [C]	P [bar]	ex [kJ/kg]	T [C]	P [bar]	ex [kJ/kg]
1.0	467	34.2	1274	393	20.5	1121	289	9.2	911
0.9	449	31.1	1240	376	18.6	1090	275	8.3	885
0.8	431	27.9	1204	359	16.7	1058	261	7.5	858
0.7	431	25.1	1192	360	15.0	1046	262	6.7	846
0.6	432	22.1	1179	361	13.2	1032	263	6.0	832
0.5	432	18.9	1161	361	11.3	1014	264	5.1	814
0.4	433	15.5	1138	362	9.3	991	266	4.2	791



*Table 4 – Energy commodity costs used in the calculations.*

Energy commodity	Nomenclature	Specific cost
Coal (CHP fuel)	$c_{coal}$	4.36 Euro/GJ [33]
Natural gas	$c_{NG}$	9.26 Euro/GJ [33]

*Table 5 – Production costs per litre of lignocellulosic ethanol produced in a full scale ethanol facility based on IBUS technology. Values from Larsen et al. [27].*

Cost parameter	Nomenclature	Specific cost
Enzymes cost	$c_{enz,0}$	0.14 Euro/L
Additives cost	$c_{add,0}$	0.06 Euro/L
Operation and maintenance cost	$c_{O\&M,0}$	0.09 Euro/L
Depreciation cost	$c_{I,0}$	0.07 Euro/L
By-product sales (molasses and solid biofuel)	$c_{sales,0}$	0.24 Euro/L

Table 6 – Operation characteristics and reference production values for the key operation points shown in Figure 5.

Point	CHP unit load, $\lambda$ [-]	Back-pressure operation parameter, $\alpha$ [-]	Ethanol facility heat production, $\beta$ [-]	Reference PGP power production, $\dot{P}_{ref}$ [MW]	Reference PGP DH production, $\dot{Q}_{ref}$ [MJ/s]
(1)	1.0	0.0	0.0	227.2	0.0
(2)	1.0	0.0	1.0	224.5	81.3
(3)	1.0	1.0	1.0	197.0	339.1
(4)	0.4	1.0	1.0	74.8	177.4
(5)	0.4	1.0	0.0	75.9	111.5
(6)	0.4	0.0	0.0	89.9	0.0
(a)	1.0	0.0	-	249.3	0.0
(b)	1.0	1.0	-	216.0	332.9
(c)	0.4	1.0	-	86.3	163.1
(d)	0.4	0.0	-	104.9	0.0

*Table 7 – Exergy content of biomass flows in the ethanol production per kg of straw treated. Values from Lythcke-Jørgensen et al. [22].*

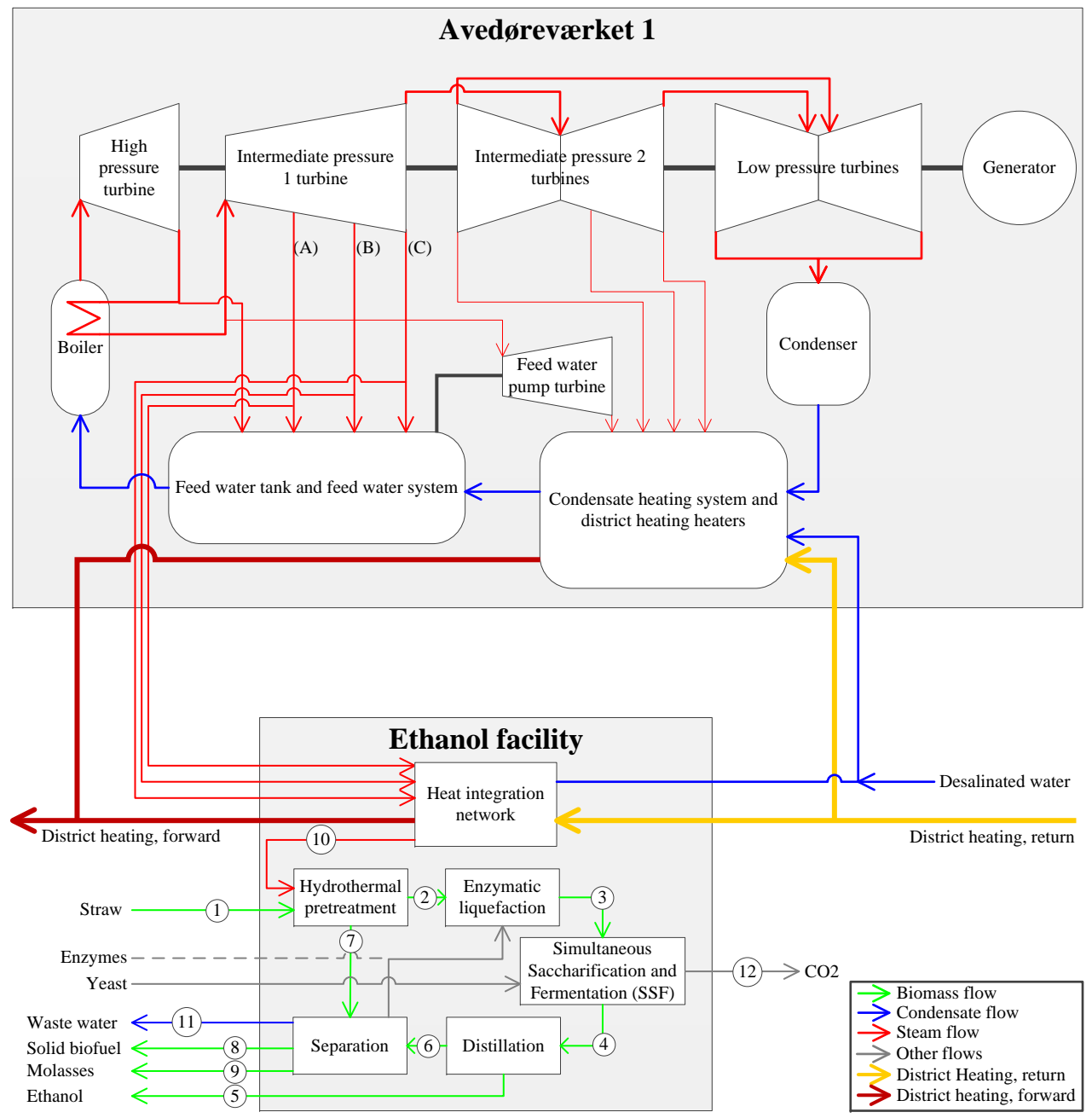
Flow description	Exergy content [MJ] – integrated operation	Exergy content [MJ] – separate operation
Straw	16.4	16.4
Natural gas	0.0	12.2
Steam	3.7 – 4.7 <sup>a</sup>	0
Fermentation broth	10.9	10.9
Liquid fraction from pretreatment	5.9	5.9
Ethanol	4.2	4.2
Molasses	4.4	4.4
Solid biofuel	8.0	8.0

<sup>a</sup> The energy consumption for the ethanol production increases with increased DH production, while the specific exergy content of extracted steam depends on operation mode of the CHP unit.

Table 8 – Exergy efficiency of the ethanol production in various operating points.

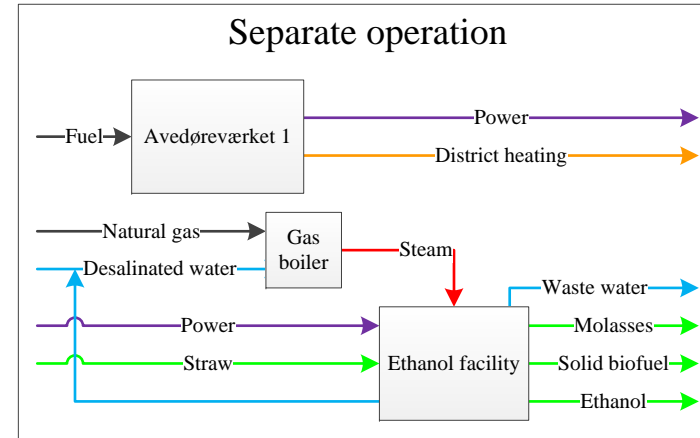
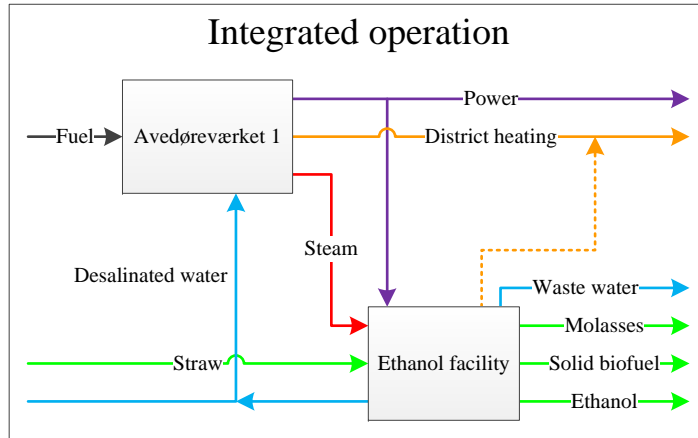
CHP Load, $\lambda_i$	Exergy efficiency, $\eta_{II}$	
	$\alpha_i = 0, \quad \beta_i = 0$	$\alpha_i = 1, \quad \beta_i = 1$
1.0	0.786	0.842
0.9	0.789	0.845
0.8	0.791	0.849
0.7	0.793	0.851
0.6	0.796	0.854
0.5	0.791	0.850
0.4	0.795	0.855
Separate operation	0.564	

Figure 1



*Figure 1 – Simplified process layout of the polygeneration plant in question. From Lythcke-Jørgensen et al. [22].*

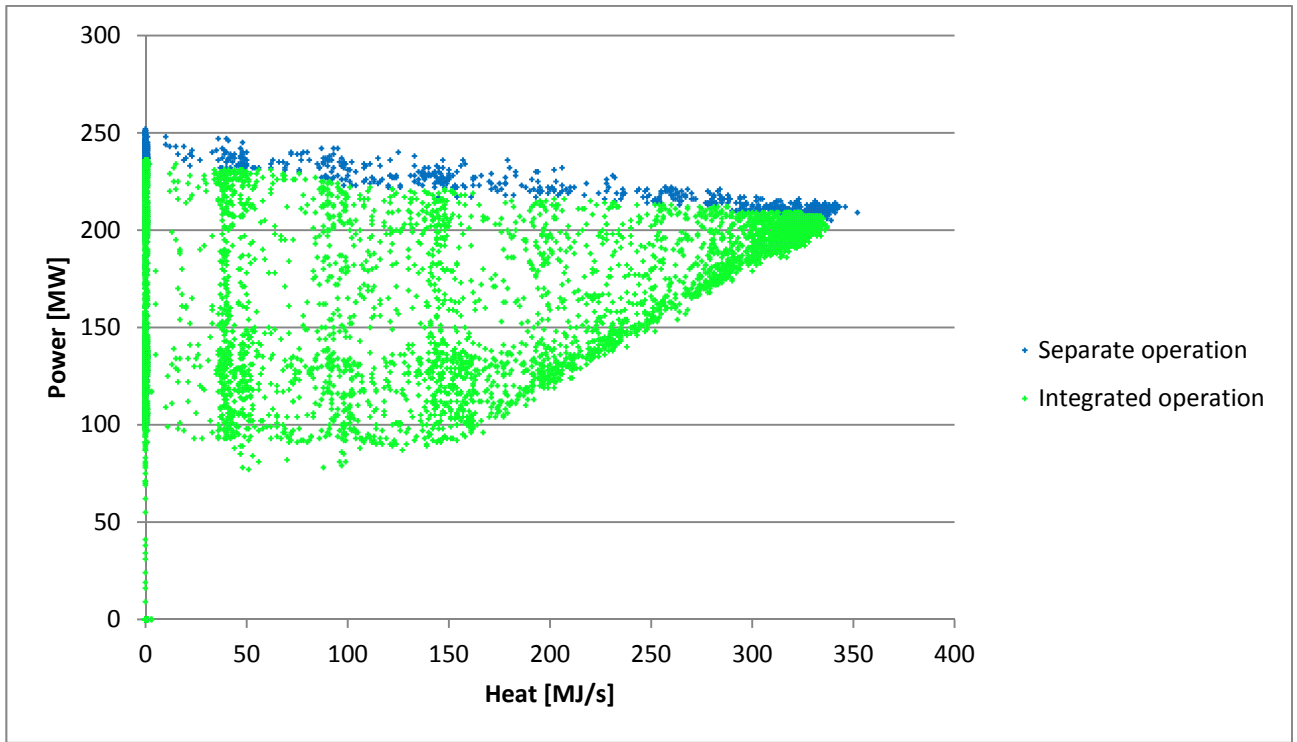
Figure 2





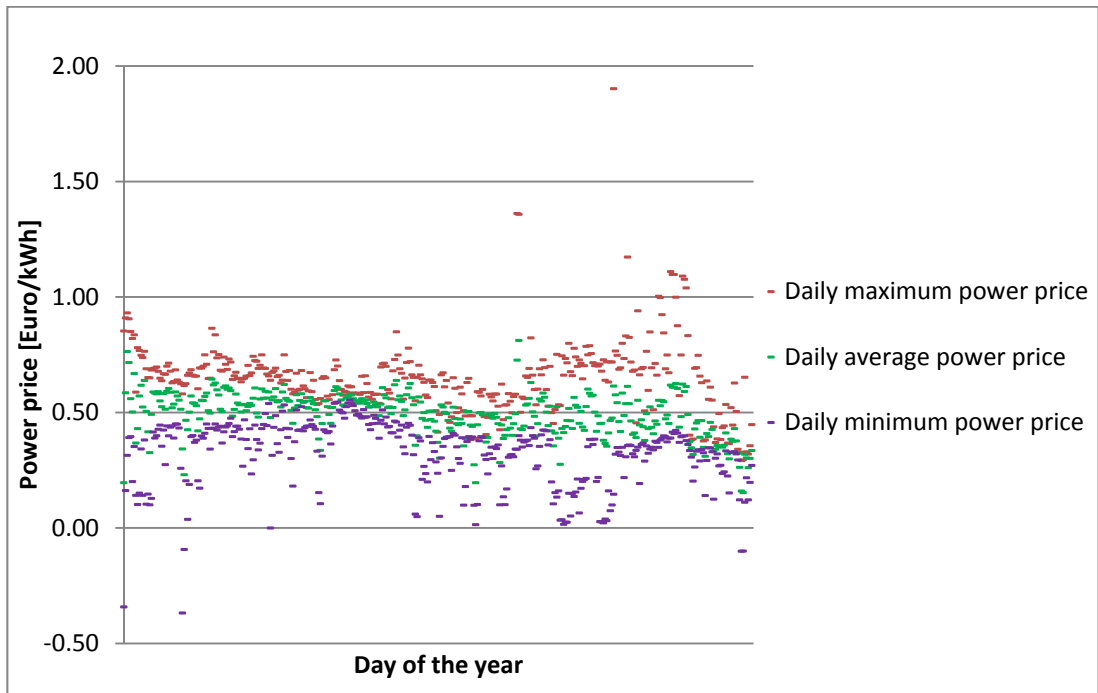
*Figure 2 – Outlines of the two operation modes in the polygeneration plant. From Lythcke-Jørgensen et al. [22].*

Figure 3



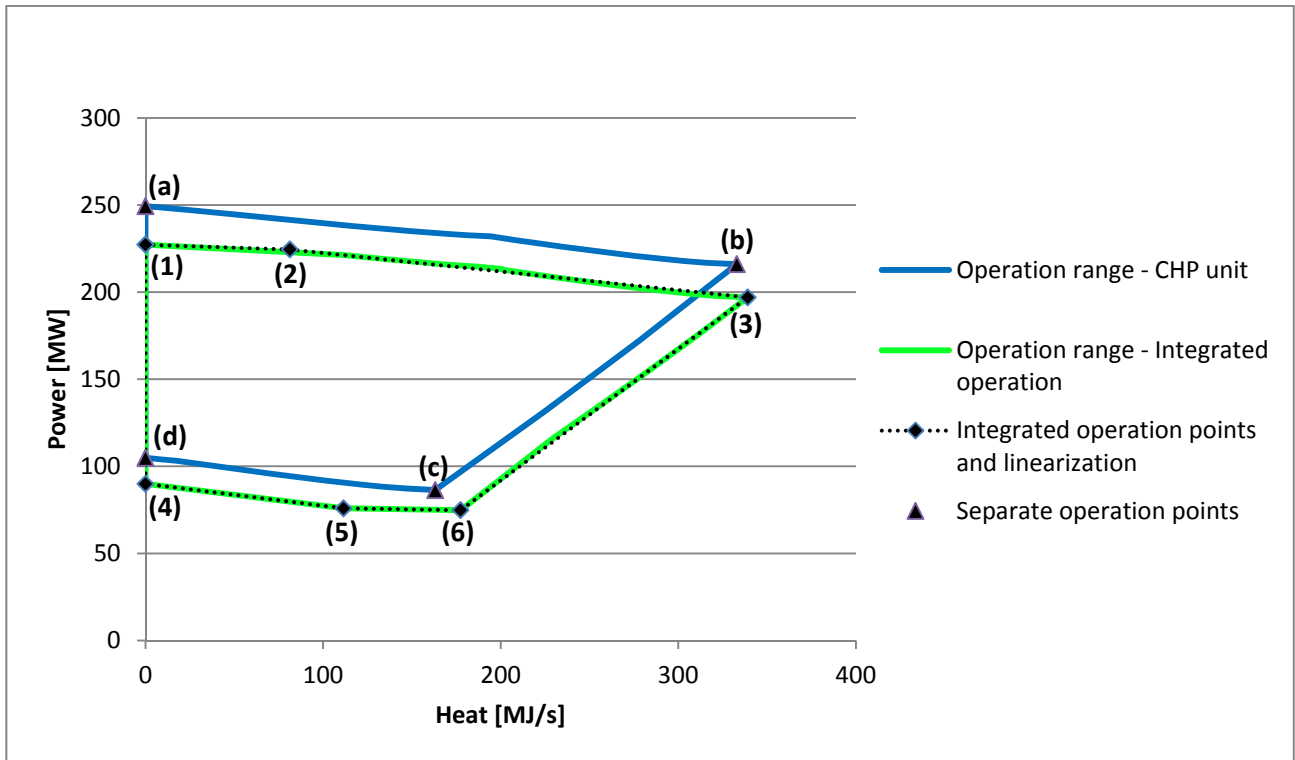
*Figure 3 – Scatter distribution of the hour-wise quasi-static operating points of the reference polygeneration plant.*

Figure 4



*Figure 4 – Scatter distribution of the daily maximum, minimum, and average electricity prices in the block 'Denmark East' in 2011.*

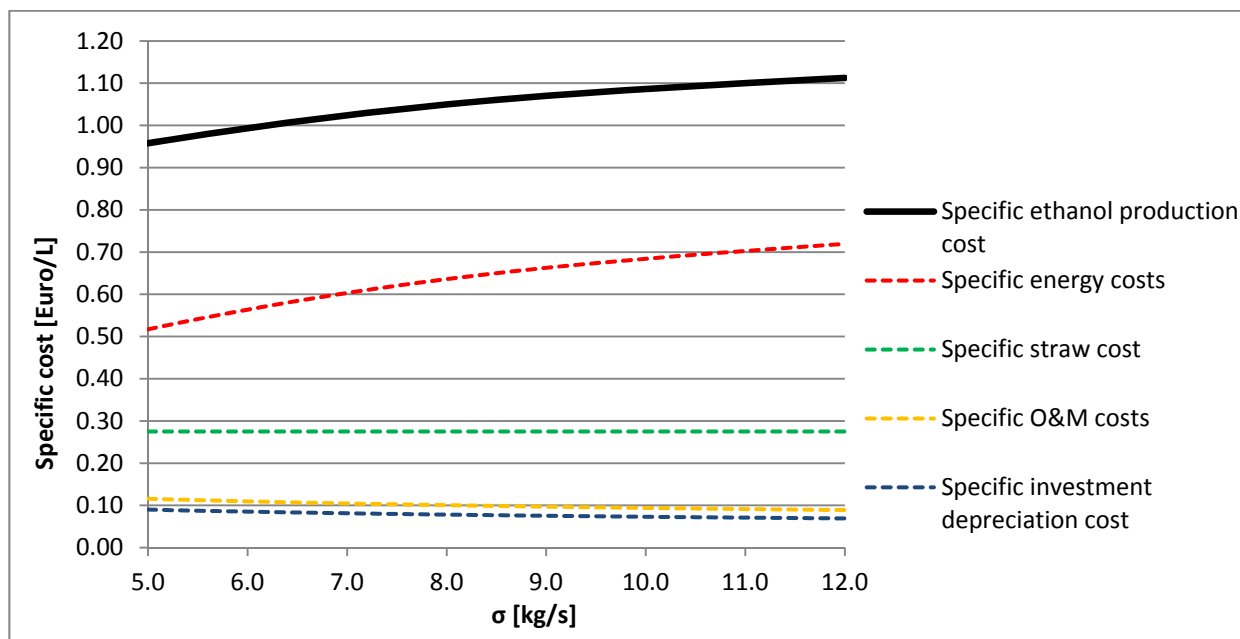
Figure 5



*Figure 5 – Operational ranges for the reference PGP in integrated and separate operation.*

*Characteristics of the six key operation points are described in Table 6.*

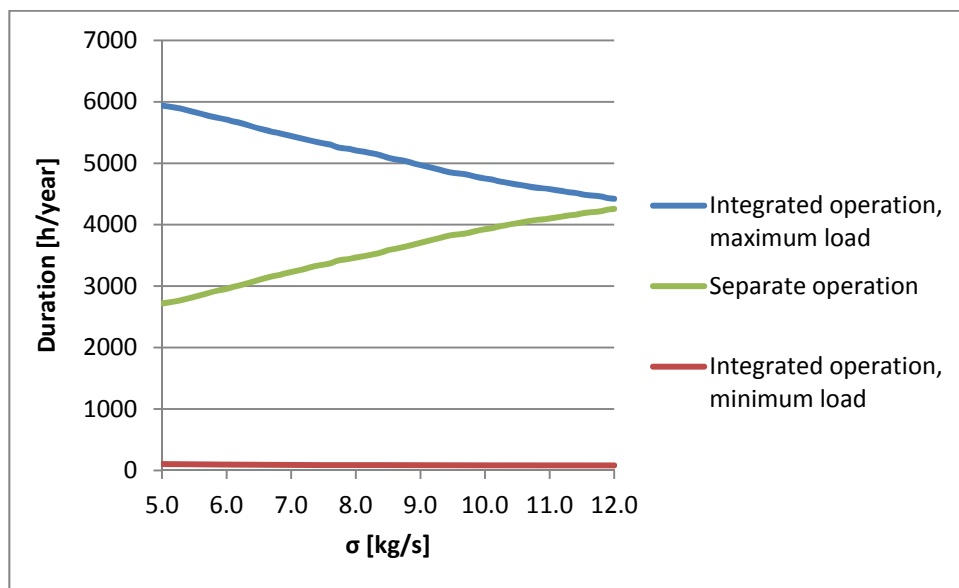
Figure 6





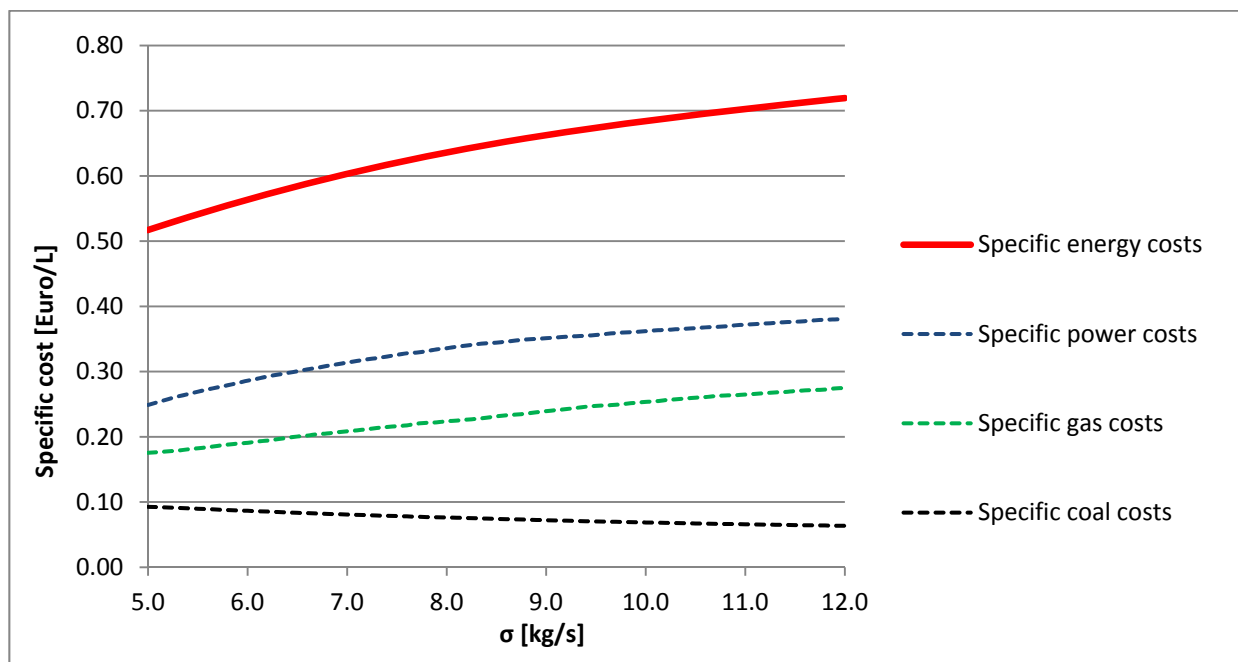
*Figure 6 – Specific ethanol production cost and important cost components as functions of  $\sigma$ .*

Figure 7



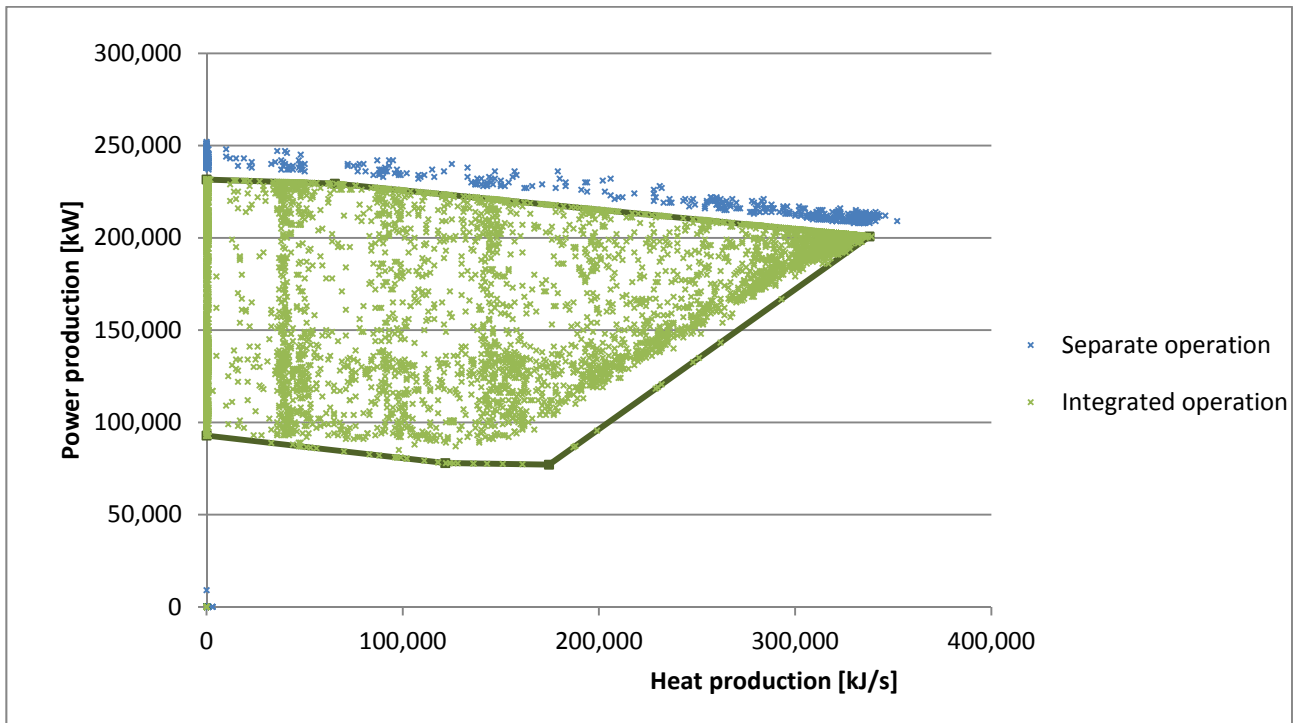
*Figure 7 – Duration of integrated and separate operation of the optimized polygeneration plant as a function of  $\sigma$ .*

Figure 8



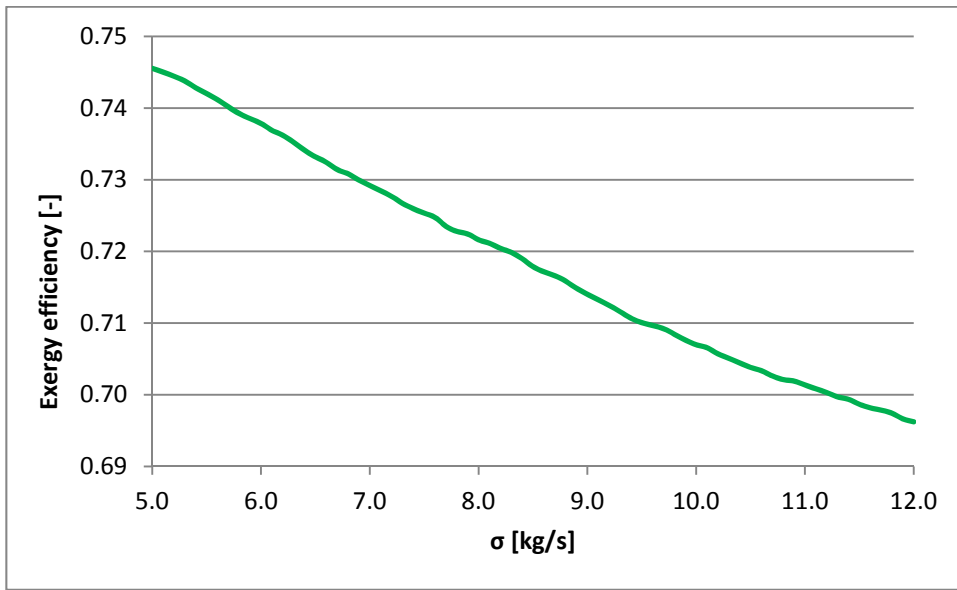
*Figure 8 – Components of the specific energy cost as functions of  $\sigma$ .*

Figure 9



*Figure 9 – Scatter distribution of hour-wise quasi-static operating points for the optimal solution.*

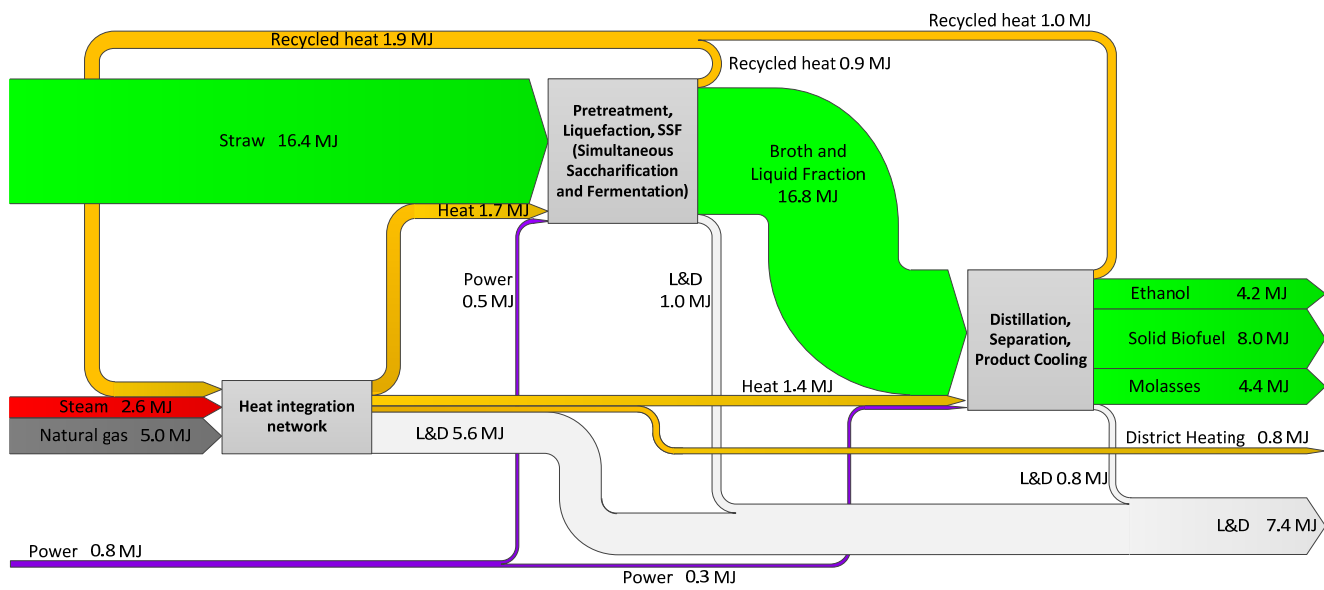
Figure 10





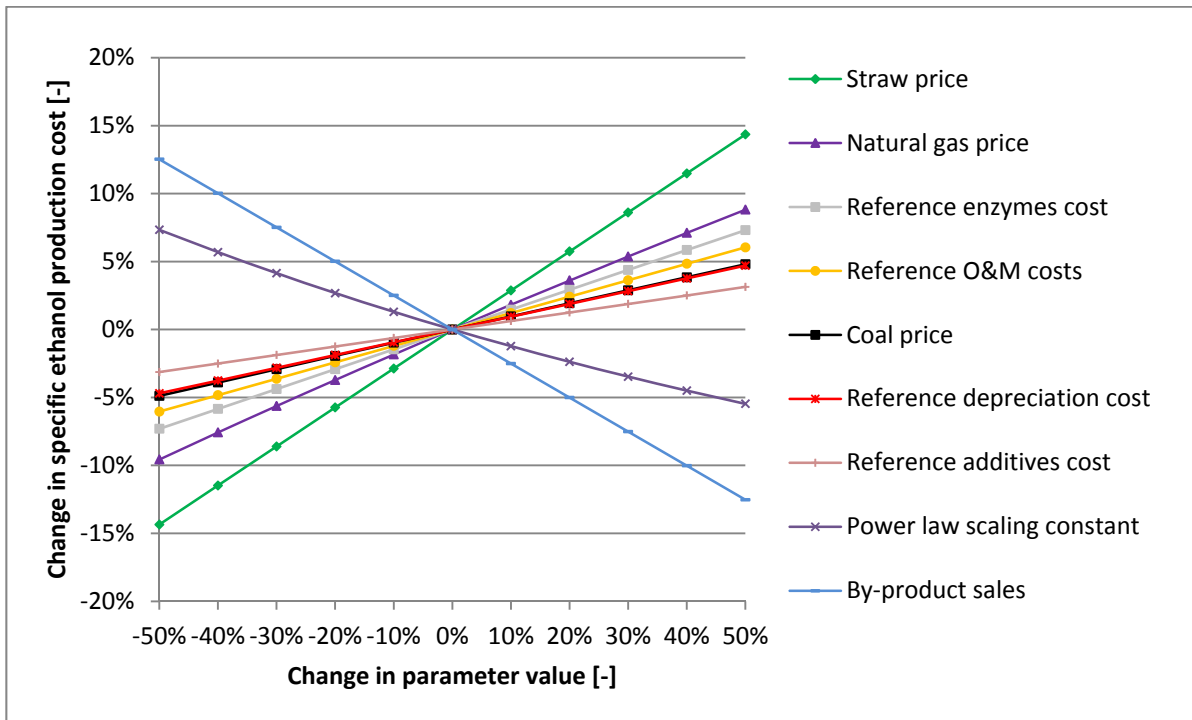
*Figure 10 – Yearly average exergy efficiency of the ethanol production at optimized operation pattern for various  $\sigma$ .*

Figure 11



*Figure 11 – Grassmann diagram illustrating yearly average exergy flows in the ethanol production for the optimal solution.*

Figure 12



*Figure 12 – Spider plot showing the impact on specific ethanol production cost from varying important parameters.*